# PruneFuse: Efficient Data Selection via Weight Pruning and Network Fusion

**Anonymous authors**
**Paper under double-blind review**

## Abstract

Efficient data selection is crucial for enhancing the training efficiency of deep neural networks and minimizing annotation requirements. Traditional methods often face high computational costs, limiting their scalability and practical use. We introduce PruneFuse, a novel strategy that leverages pruned networks for data selection and later fuses them with the original network to optimize training. PruneFuse operates in two stages: First, it applies structured pruning to create a smaller pruned network that, due to its structural coherence with the original network, is well-suited for the data selection task. This small network is then trained and selects the most informative samples from the dataset. Second, the trained pruned network is seamlessly fused with the original network. This integration leverages the insights gained during the training of the pruned network to facilitate the learning process of the fused network while leaving room for the network to discover more robust solutions. Extensive experimentation on various datasets demonstrates that PruneFuse significantly reduces computational costs for data selection, achieves better performance than baselines, and accelerates the overall training process.

## 1 Introduction

Deep learning models have achieved remarkable success across various domains, ranging from image recognition to natural language processing (Ren et al., 2015; Long et al., 2015; He et al., 2016). However, the performance of models heavily relies on the access to large amounts of labeled data for training (Sun et al., 2017). In practical real-world applications, manually annotating massive datasets can be prohibitively expensive and time-consuming. Data selection techniques such as Active Learning (AL) (Gal et al., 2017) offer a promising solution to this challenge by iteratively selecting the most informative samples from the unlabeled dataset for annotation, thereby reducing labeling costs while approaching or even surpassing the performance of fully supervised training. Even with the rapid scaling of large language models and multimodal foundation models, effective adaptation to downstream tasks continues to demand high-quality, domain-aligned labeled data. A growing body of work demonstrates that principled selection techniques, including AL, outperform simple scaling of in-domain data in both final performance and overall computational efficiency (Xie et al., 2023; Yu et al., 2024; 2025). Traditional AL methods, however, incur severe computational overhead. Each selection cycle in AL typically requires extensive training or inference with a large model on the entire unlabeled pool. As model and dataset sizes grow, this repeated training becomes a critical scalability bottleneck, especially in resource-constrained environments. In this paper, we propose a novel strategy for efficient data selection in an AL setting that overcomes the limitations of traditional approaches. Our approach builds on the concept of model pruning, which selectively reduces the complexity of neural networks while preserving their accuracy. By utilizing small pruned networks as reusable data selectors, we eliminate the need to train large models, specifically during the data selection phase, thus significantly reducing computational demands. By enabling swift identification of the most informative samples, our method not only enhances the efficiency of AL but also ensures its scalability and cost-effectiveness in resource-limited settings. Additionally, we employ these pruned networks to train the final model through a fusion process, effectively harnessing the insights from the trained networks to accelerate convergence and improve generalization.

**Main Contribution.** To summarize, our key contribution is to introduce PruneFuse, an efficient and rapid data selection technique that leverages pruned networks. This approach mitigates the need for continuous training of a large model prior to data selection, which is inherent in conventional active learning methods. By employing pruned networks as data selectors, PruneFuse ensures computationally efficient selection of informative samples, which leads to overall superior generalization. Furthermore, we propose the novel concept of fusing these pruned networks with the original untrained model, enhancing model initialization and accelerating convergence during training.

We demonstrate the broad applicability of PruneFuse across various network architectures, providing researchers and practitioners with a flexible tool for efficient data selection in diverse deep learning settings. Extensive experimentation on CIFAR-10, CIFAR-100, Tiny-ImageNet-200, ImageNet-1K, text datasets (Amazon Review Polarity and Amazon Review Full), as well as Out-of-Distribution (OOD) benchmarks, shows that PruneFuse achieves superior performance to state-of-the-art AL methods while significantly reducing computational costs.

## 2 Related Work

**Data Selection.** Recent studies have explored techniques to improve the efficiency of data selection in deep learning. Approaches such as coreset selection (Sener & Savarese, 2018a), BatchBALD (Kirsch et al., 2019), and Deep Bayesian Active Learning (Gal et al., 2017) aim to select informative samples using techniques like diversity maximization and Bayesian uncertainty estimation. Parallelly, the domain of active learning has unveiled strategies, such as uncertainty sampling (Shen et al., 2018; Sener & Savarese, 2018b; Kirsch et al., 2019), expected model change-based approach (Freytag et al., 2014; Käding et al., 2016), snapshot ensembles Jung et al. (2023), and query-by-density (Sener & Savarese, 2018a). These techniques prioritize samples that can maximize information gain, thereby enhancing model performance with minimal labeling effort. While these methods achieve efficient data selection, they still require training large models for the selection process, resulting in significant computational overhead. Other strategies, such as Gradient Matching (Killamsetty et al., 2021a) optimize this selection process by matching the gradients of a subset with the training or validation set based on the orthogonal matching algorithm, and (Killamsetty et al., 2021b) performs meta-learning based approach for online data selection. SubSelNet (Jain et al., 2023) proposes to approximate a model that can be used to select the subset for various architectures without retraining the target model, hence reducing the overall overhead. However, it involves a pre-training routine, which is very costly and must be repeated for any change in data or model distribution. SVP (Coleman et al., 2020) introduces using small proxy models for data selection, however, after selection, the proxy is discarded and the target model is trained from scratch on the chosen subset. Additionally, structural discrepancies between the proxy and target models may result in suboptimal data selections. Our approach also builds on this foundation of using a small model (which in our case is a pruned model), but it enables direct integration with the target model through the fusion process. This ensures that the knowledge acquired during data selection is retained and actively contributes to the training of the original model. Also, the architectural coherence between the pruned and the target model provides a more seamless and effective mechanism for data selection, enhancing overall model performance and efficiency.

**Efficient Deep Learning.** Efficient deep learning has gained significant attention in recent years. Methods such as Neural Architecture Search (NAS) (Zoph & Le, 2016; Wan et al., 2020), network pruning (Han et al., 2016), quantization (Dong et al., 2020; Jacob et al., 2018; Zhou et al., 2016), and knowledge distillation (Hinton et al., 2015; Yin et al., 2020) have been proposed to reduce model size and computational requirements. Neural Network pruning has been extensively investigated as a technique to reduce the complexity of deep neural networks (Han et al., 2016). Pruning strategies can be broadly divided into Unstructured Pruning (Dong et al., 2017; Guo et al., 2016; Park et al., 2020) and Structured Pruning (Li et al., 2016; He et al., 2017; You et al., 2019; Ding et al., 2019) based on the granularity and regularity of the pruning scheme. Unstructured pruning often yields a superior accuracy-size trade-off, whereas structured pruning offers practical speedup and compression without necessitating specialized hardware. While pruning literature suggests pruning after training (Renda et al., 2020) or during training (Zhu & Gupta, 2017; Gale et al., 2019), recent research explores the viability of pruning at initialization (Lee et al., 2019; Tanaka et al., 2020; Frankle et al., 2021; Wang et al., 2020). In our work, we leverage the benefits of model pruning at initialization

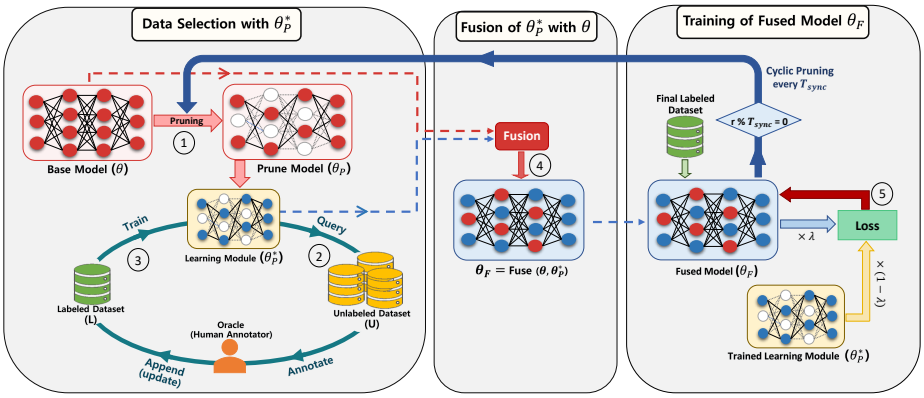


Figure 1: **Overview of the PruneFuse method**: (1) An untrained neural network is initially pruned to form a structured, pruned network $\theta_p$. (2) This pruned network $\theta_p$ queries the dataset to select prime candidates for annotation, similar to active learning techniques. (3) $\theta_p$ is then trained on these labeled samples to form the trained pruned network $\theta_p^*$. (4) The trained pruned network $\theta_p^*$ is fused with the base model $\theta$, resulting in a fused model. (5) The fused model is further trained on a selected subset of the data, incorporating knowledge distillation from $\theta_p^*$. At regular intervals $T_{\text{sync}}$, the fused model is utilized to dynamically update the pruned model for subsequent data selection.

to create a small representative model for efficient data selection, allowing for the rapid identification of informative samples while minimizing computational requirements.

## 3 Background and Motivation

Efficient data selection is paramount in modern machine learning applications, especially when dealing with deep neural networks. The subset selection problem can be framed as the challenge of selecting a subset $s$ from a dataset $D = (x_i, y_i)_{i=1}^n$ such that a model $\theta$ trained on $s$ approximates the performance of the same model trained on the full dataset,

$$\arg\min_s \left| E_{(x,y)\in s}[l(x,y;\theta)] - E_{(x,y)\in D}[l(x,y;\theta)] \right| \tag{1}$$

where $E_{(x,y)\in s}[l(x,y;\theta)]$ is the expected loss on the selected subset $s$ and $E_{(x,y)\in D}[l(x,y;\theta)]$ is the expected loss on the entire dataset.

### 3.1 Subset Selection Framework

Active Learning (AL) is a widely utilized iterative approach tailored for situations with abundant unlabeled data. Given a classification task with $C$ classes and a large pool of unlabeled samples $U$, AL revolves around selectively querying the most informative samples from $U$ for labeling. The process commences with an initial set of randomly sampled data $s^0$ from $U$, which is subsequently labeled. In subsequent rounds, AL augments the labeled set $L$ by adding newly identified informative samples. This cycle repeats until a predefined number of labeled samples, denoted by $b$, has been selected.

### 3.2 Network Pruning and Its Relevance

Network pruning emerges as a potent tool to reduce the complexity of neural networks. By eliminating redundant parameters, pruning preserves vital network functionalities while streamlining its architecture. Pruning strategies can be broadly categorized into Unstructured Pruning and Structured Pruning. Unstructured Pruning targets the removal of individual weight independent of their location. While it trims down the overall number of parameters, tangible computational gains on conventional hardware often demand very high pruning ratios (Park et al., 2017). On the other hand, Structured Pruning emphasizes the removal of larger constructs like kernels, channels, or layers. Its strength lies in preserving locally dense computations, which not only yields a leaner network but also bestows immediate performance improvements (Liu et al., 2017). Given its computational benefits, particularly in expediting evaluations and aligning with hardware optimizations, we opted for Structured Pruning over its counterpart. Importantly, pruned networks maintain

the architectural coherence of the original model. This coherence makes them inherently more suitable for tasks such as data selection. Unlike heavily modified or entirely different models that can be used for data selection Coleman et al. (2020); Jain et al. (2023), the pruned model echoes the original structure, particularly advantageous in recognizing and prioritizing data samples that resonate with the patterns of the original network. The goal is clear: to develop a data selection strategy that conserves computational resources, minimizes memory overhead, and potentially improves model generalization.

## 4 PruneFuse

In this section, we delineate the PruneFuse methodology. The procedure begins with network pruning at initialization, offering a streamlined model for data selection. Upon attaining the desired data subset, the pruned model undergoes a fusion process with the original network, leveraging the structural coherence between them. The fused model is subsequently refined through knowledge distillation, enhancing its performance. An overall view of our proposed methodology is illustrated in Fig. 1. We modify the problem in Eq. 1 as follows.

Let $s_p$ be the subset selected using a pruned model $\theta_p$ and $s$ be the subset selected using the original model $\theta$. We want to minimize:

$$\arg\min_{s_p} \left| E_{(x,y)\in s_p}[l(x,y;\theta,\theta_p)] - E_{(x,y)\in D}[l(x,y;\theta)] \right| \tag{2}$$

where $E_{(x,y)\in s_p}[l(x,y;\theta,\theta_p)]$ is the expected loss on subset $s_p$ (selected using $\theta_p$) when evaluated using the original model $\theta$ and $E_{(x,y)\in D}[l(x,y;\theta)]$ is the expected loss on full dataset $D$ when trained using the original model $\theta$. Furthermore, the subset can be defined as $s_p = \{(x_i, y_i) \in D \mid \text{score}(x_i, y_i; \theta_p) \geq \tau\}$ where $\text{score}(x_i, y_i; \theta_p)$ represents the acquisition score assigned to each sample selected using $\theta_p$. The score function can be based on various strategies such as Least Confidence, Entropy, or Greedy k-centers. $\tau$ defines the threshold used in the score-based selection methods (Least Confidence or Entropy) to determine the inclusion of a sample in $s_p$.

The goal of the optimization problem is to select $s_p$ from the full dataset $D$ such that when $\theta$ is trained on it, the performance is as close as possible to training $\theta$ on $D$. Algorithm 1 precisely describes the PruneFuse methodology. The key insight is that the subset $s_p$ is selected using the lightweight pruned model $\theta_p$ and is sufficiently representative and informative for training the original model $\theta$ due to strong structural coherence between $\theta$ and $\theta_p$, ensuring that the selection made by $\theta_p$ effectively minimizes the loss when $\theta$ is trained on $s_p$.

### 4.1 Pruning at Initialization

Pruning at initialization has been demonstrated to uncover superior solutions compared to the conventional approach of pruning an already trained network followed by fine-tuning (Wang et al., 2020). Specifically, it shows potential in training time reduction and enhanced model generalization. In our methodology, we employ structured pruning due to its benefits, such as maintaining the architectural coherence of the network, enabling more predictable resource savings, and often leading to better-compressed models in practice.

Consider an untrained neural network, represented as $\theta$. Let each layer $\ell$ of this network have feature maps or channels denoted by $c^\ell$, with $\ell \in \{1, \ldots, L\}$. Channel pruning results in binary masks $m^\ell \in \{0,1\}^{d^\ell}$ for every layer, where $d^\ell$ represents the total number of

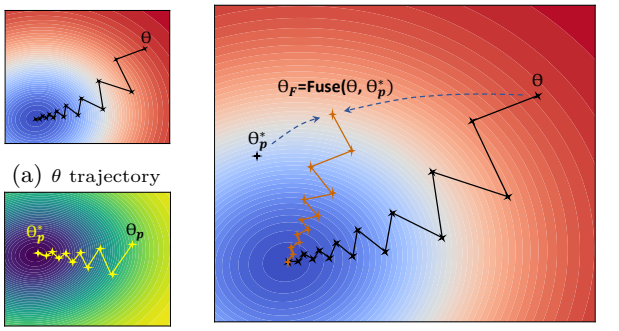


(a) $\theta$ trajectory

(b) $\theta_p$ trajectory

(c) $\theta_F$ with a refined trajectory due to fusion

Figure 2: **Evolution of training trajectories**. Pruning $\theta$ to $\theta_p$ tailors the loss landscape from 2a to 2b, allowing $\theta_p$ to converge on an optimal configuration, denoted as $\theta_p^*$. This model, $\theta_p^*$, is later fused with the original $\theta$, which provides better initialization and offer superior trajectory for $\theta_F$ to follow, as depicted in 2c.

channels in layer $\ell$. The pruned subnetwork, $\theta_p$, retains channels described by $c^\ell \odot m^\ell$, where $\odot$ symbolizes the element-wise product. The sparsity $p \in [0, 1]$ of the subnetwork illustrates the proportion of channels that are pruned: $p = 1 - \sum_\ell m^\ell / \sum_\ell d^\ell$.

To reduce the model complexity, we employ the channel pruning procedure $prune(C, p)$. This prunes to a sparsity $p$ via two primary functions: i) score(C): This operation assigns scores $z^\ell \in \mathbb{R}^{d^\ell}$ to every channel in the network contingent on their magnitude (using the L2 norm). The channels $C$ are represented as $(c_1, \ldots, c_L)$. and ii) remove(Z, p): This process takes the magnitude scores $Z = (z_1, \ldots, z_L)$ and translates them into masks $m^\ell$ such that the cumulative sparsity of the network, in terms of channels, is $p$. We employ a one-shot channel pruning that scores all the channels simultaneously based on their magnitude and prunes the network from 0% sparsity to $p$% sparsity in one cohesive step. Although previous works suggest re-initializing the network to ensure proper variance (van Amersfoort et al., 2020), the performance gains are marginal; we retain the weights of the pruned network before training.

### 4.2 Data Selection via Pruned Model

We begin by randomly selecting a small subset of data samples, denoted as $s^0$, from the unlabeled pool $U = \{x_i\}_{i \in [n]}$ where $[n] = \{1, ..., n\}$. These samples are then annotated. The pruned model $\theta_p$ is trained on this labeled subset $s^0$, resulting in the trained pruned model $\theta_p^*$. At each subsequent round, $\theta_p^*$ scores $U$ and proposes a batch of $k$ points for annotation.

We instantiate three widely used criteria for data selection, namely Least Confidence (LC) (Settles, 2012), Entropy (Shannon, 1948), and Greedy k-centers (Sener & Savarese, 2018a).

1. Least Confidence based selection tends toward samples where the pruned model exhibits the least confidence in its predictions. The confidence score is essentially the highest probability the model assigns to any class label. Thus, the uncertainty score for a given sample $x_i$ based on LC is defined as $\text{score}(x_i; \theta_p^*)_{\text{LC}} = 1 - \max_{\hat{y}} P(\hat{y}|x_i; \theta_p^*)$. 2. In Entropy based selection, the entropy of the model's predictions is the focal point. Samples with high entropy indicate situations where $\theta_p^*$ is ambivalent about the correct label. For each sample in $U$, the uncertainty based on entropy is computed as $\text{score}(x_i; \theta_p^*)_{\text{Entropy}} = -\sum_{\hat{y}} P(\hat{y}|x_i; \theta_p^*) \log P(\hat{y}|\mathbf{x}_i; \theta_p^*)$. Subsequently, we select the top-$k$ samples exhibiting the highest uncertainty scores, proposing them as prime candidates for annotation. 3. The objective of the Greedy k-centers algorithm is to cherry-pick $k$ centers from the dataset such that the maximum distance of any sample from its nearest center is minimized. The algorithm proceeds in a greedy manner by selecting the first center arbitrarily and then iteratively selecting the next center as the point that is furthest from the current set of centers. The selection can be mathematically represented as $x = \arg\max_{x \in U} \min_{c \in \text{centers}} d(x, c)$ where centers is the current set of chosen centers and $d(x, c)$ is the distance between point $x$ and center $c$. Although various metrics can be used to compute this distance, we opt for the Euclidean distance since it is widely used in this context.

**Algorithm 1** PruneFuse

**Input**: Unlabeled dataset $U$, initial labeled data $s^0$, labeled dataset $L$, original model $\theta$, prune model $\theta_p$, fuse model $\theta_F$, pruning ratio $p$, AL rounds $R$ to achieve budget $b$, synchronization interval $T_{sync}$, and scored $j^{th}$ data sample $D_j$

```
Randomly initialize θ
θ_p ← Prune(θ, p) //structured pruning
θ*_p ← Train(θ_p, s^0)
L ← s^0
for r = 1 to R do
    Compute score(x; θ*_p) ∀ x ∈ U
    D_k = top_k[D_j ∈ U]_{j∈[k]}
    Query labels y_k for selected samples D_k
    L ← L ∪ {(D_k, y_k)}
    if T_sync = 0 or r%T_sync != 0 then
        θ*_p ← Train(θ_p, L)
    else if r%T_sync = 0 then
        θ*_F ← Fuse(θ, θ*_p) and Fine-tune on L
        θ*_p ← Prune(θ*_F, p) and Fine-tune on L
θ_F ← Fuse(θ, θ*_p)
θ*_F ← Fine-tune θ_F on L
Return L, θ*_F
```

*Remark.* These criteria are standard, and our contributions are orthogonal to the choice of acquisition score. Alternative or learned scores can be seamlessly integrated into our pipeline; see Supplementary Materials 8.4, 8.12 for more details.

### 4.3 Training of Pruned Model

Once we have selected the samples from $U$, they are annotated to get their respective labels. These freshly labeled samples are assimilated into the labeled dataset $L$. At the start of each training cycle, a fresh pruned model $\theta_p$ is generated. Training from scratch in every iteration is vital to prevent the model from developing spurious correlations or overfitting to specific samples (Coleman et al., 2020). This further ensures that the model learns genuine patterns in the updated labeled dataset without carrying over potential biases from previous rounds. The training process adheres to a typical deep learning paradigm. Given the dataset $L$ with samples $(x_i, y_i)$, the aim is to minimize the loss function: $\mathcal{L}(\theta_p, L) = \frac{1}{|L|}\sum_{i=1}^{|L|}\mathcal{L}_i(\theta_p, x_i, y_i)$, where $\mathcal{L}_i$ denotes the individual loss for the sample $x_i$. Training unfolds over multiple iterations (or epochs). In each iteration, the weights of $\theta_p$ are updated using backpropagation with an optimization algorithm such as stochastic gradient descent (SGD).

This process is inherently iterative, as in standard Active Learning. After each round of training, new samples are chosen, annotated, and the model is reinitialized and retrained from scratch. This cycle persists until certain stopping criteria, e.g., labeling budget or desired performance, are met. With the incorporation of new labeled samples at every stage, $\theta_p^*$ progressively refines its performance, becoming better suited for the subsequent data selection phase.

### 4.4 Fusion with the Original Model

After achieving the predetermined budget, the next phase is to integrate the insights from the trained pruned model $\theta_p^*$ into the untrained original model $\theta$. This step is crucial, as it amalgamates the learned knowledge from the pruned model with the expansive architecture of the original model, aiming to harness the best of both worlds.

**Rationale for Fusion.** Traditional pruning and fine-tuning methods often involve training a large model, pruning it down, and then fine-tuning the smaller model. While this is effective, it does not fully exploit the potential benefits of the larger, untrained model. The primary reason is that the pruning process might discard useful structures and connections within the original model that were not yet leveraged during initial training. By fusing the trained pruned model with the untrained original model, we aim to create a model that combines the learned knowledge by $\theta_p^*$ with the broader, unexplored model $\theta$.

**The Fusion Process.** Fusion transfers the trained parameters of the pruned selector $\theta_p^*$ into the *corresponding coordinates* of the original (untrained) dense model $\theta$, producing the fused model,

$$\theta_F = \mathrm{Fuse}(\theta, \theta_p^*).$$

We view $\theta$ as a sequence of layers $j = 1, \ldots, L$. For each layer $j$, structured pruning at initialization selects a subset of output-channel indices $I_j \subseteq \{1, \ldots, C_{\mathrm{out}}^{(j)}\}$ and, by architectural coherence, the pruned layer $\theta_p^*$ is isomorphic to the sub-tensor of the dense layer indexed by $[I_j \times I_{j-1}]$ (with $I_0 = \{1, \ldots, C_{\mathrm{in}}^{(1)}\}$, e.g., RGB channels).

*Convolutional layers.* Let $W^{(j)} \in \mathbb{R}^{C_{\mathrm{out}}^{(j)} \times C_{\mathrm{in}}^{(j)} \times k_h \times k_w}$ denote the dense weights of layer $j$, and $W_{p^*}^{(j)} \in \mathbb{R}^{|I_j| \times |I_{j-1}| \times k_h \times k_w}$ the trained pruned weights. The weight-aligned fusion copies the trained sub-tensor into the matching coordinates of the dense tensor and keeps all remaining entries at their initial values:

$$\begin{aligned} W_F^{(j)}[I_j, I_{j-1}, :, :] &\leftarrow W_{p^*}^{(j)}, \\ W_F^{(j)}[I_j, \overline{I}_{j-1}, :, :] &\leftarrow W_{\mathrm{init}}^{(j)}[I_j, \overline{I}_{j-1}, :, :], \\ W_F^{(j)}[\overline{I}_j, :, :, :] &\leftarrow W_{\mathrm{init}}^{(j)}[\overline{I}_j, :, :, :], \end{aligned}$$

with the same coordinate replacement for biases (if present) and normalization parameters $(\gamma, \beta, \mu, \sigma^2)$ on the indices $I_j$.

*Linear layers.* For $W^{(j)} \in \mathbb{R}^{C_{\text{out}}^{(j)} \times C_{\text{in}}^{(j)}}$, the output dimension (e.g., number of classes) is unchanged; fusion aligns on the input channels:

$$W_F^{(j)}[:, I_{j-1}] \leftarrow W_{p^*}^{(j)}, \qquad W_F^{(j)}[:, \overline{I}_{j-1}] \leftarrow W_{\text{init}}^{(j)}[:, \overline{I}_{j-1}].$$

Instead of a coordinate copy, one may spread the trained pruned weights across multiple dense coordinates via a layer-wise dispersion map $D_j$:

$$W_F^{(j)} \leftarrow \underbrace{D_j\big(W_{p^*}^{(j)}\big)}_{\text{expanded onto } (C_{\text{out}}^{(j)}, C_{\text{in}}^{(j)})} \odot \mathbf{M}_j \; + \; W_{\text{init}}^{(j)} \odot (1 - \mathbf{M}_j),$$

where $\mathbf{M}_j$ is a binary mask that indicates where the dispersed weights land.

**Advantages of Retaining Unaltered Weights.** By copying the weights from the trained pruned model $\theta_p^*$ into their corresponding locations within the untrained original model $\theta$, and leaving the remaining weights of $\theta$ yet to be trained, we create a unique blend. The weights from $\theta_p^*$ encapsulate the knowledge acquired during training, providing a foundation. Meanwhile, the rest of the untrained weights in $\theta$ still have their initial values, offering an element of randomness. This duality fosters a richer exploration of the loss landscape during subsequent training. Fig. 2 illustrates the transformation in training trajectories resulting from the fusion process. The trained weights of $\theta_p^*$ provide better initialization, while the unaltered weights serve as gateways to unexplored regions in the loss landscape. As we show in Section 6, this strategic combination in the fused model $\theta_F$ offers a better solution than the pruned or the original model alone.

### 4.5 Refinement via Knowledge Distillation

Based on the discussed strategy above, we show that PruneFuse outperforms baseline AL (results provided in the Supplementary Materials 8.6). However, to further optimize, we fine-tune $\theta_F$ using Knowledge Distillation (KD) with soft logits from the pruned network. KD enables $\theta_F$ to learn from $\theta_p^*$ (the teacher model), enriching its training. During the fine-tuning phase, we use two losses: i) Cross-Entropy Loss, which quantifies the divergence between the predictions of $\theta_F$ and the actual labels in dataset $L$, and ii) Distillation Loss, which measures the difference in the softened logits of $\theta_F$ and $\theta_p^*$. These softened logits are derived by tempering logits of $\theta_p^*$, which in our case is the teacher model, with a temperature parameter before applying the softmax function. The composite loss for the fine-tuning phase is formulated as a weighted average of both losses. The iterative enhancement of $\theta_F$ is governed by: $\theta_F^{(t+1)} = \theta_F^{(t)} - \alpha \nabla_{\theta_F^{(t)}} (\lambda \mathcal{L}_{\text{Cross Entropy}}(\theta_F^{(t)}, L) + (1 - \lambda)\mathcal{L}_{\text{Distillation}}(\theta_F^{(t)}, \theta_p^*))$. Here, $\alpha$ represents the learning rate, while $\lambda$ functions as a coefficient to balance the contributions of the two losses. Incorporating KD in the fine-tuning phase aims to harness the insights of the pruned model $\theta_p^*$. By doing so, our objective is to ensure that the fused model $\theta_F$ not only retains the trained weights of the pruned model but also reinforces this knowledge iteratively, optimizing the performance of $\theta_F$ in subsequent tasks.

### 4.6 Iterative Pruning of Fused Model

PruneFuse introduces a strategy to dynamically update the pruned model, $\theta_p$, from the trained fused model $\theta_F^*$ at predefined intervals $T_{\text{sync}}$. In each AL cycle, the pruned model $\theta_p$, obtained by pruning a randomly initialized network, is trained on the labeled dataset $L$ and subsequently employed to score the unlabeled data $U$. At every $T_{\text{sync}}$ cycle, the pruned model $\theta_p$ is obtained by pruning the trained fused model $\theta_F^*$, which is then fine-tuned with $L$ to get $\theta_p^*$ and later employed to score the $U$ in the subsequent rounds. By periodically synchronizing the pruned model with the fused model at regular $T_{\text{sync}}$ intervals, PruneFuse effectively balances computational efficiency with data selection precision. This iterative refinement process enables the pruned model to leverage the robust architecture of the fused model, allowing it to evolve dynamically with each cycle and leading to continuous performance improvements. As a result, PruneFuse achieves a better trade-off between accuracy and efficiency, enhancing the AL process while maintaining computational viability.

## 5 Error Bound for PruneFuse

**Assumption 5.1.** *The loss function $l(x, y; \theta)$ is Lipschitz continuous with respect to the model parameters $\theta$, with constant $L$:*

$$|l(x, y; \theta_1) - l(x, y; \theta_2)| \leq L\|\theta_1 - \theta_2\| \tag{3}$$

**Assumption 5.2.** *The pruned subset $s_p$ is selected using the pruned model $\theta_p$ using an acquisition score (e.g. Least Confidence or Entropy), and the expected loss over $s_p$ approximates that over $D$ with probability at least $1 - \eta$ (over the randomness of the selection rule). Specifically,*

$$\left|\mathbb{E}_{(x,y)\in s_p}[l(x, y; \theta_p)] - \mathbb{E}_{(x,y)\in D}[l(x, y; \theta_p)]\right| \leq \delta \tag{4}$$

*Thus the subset yields a $\delta$–accurate estimate of the population loss.*

**Assumption 5.3.** *After each synchronization step, the pruned model $\theta_p$ is derived from the full model $\theta$. Specifically, each fusion step contracts the gap by a factor $\alpha$:*

$$\|\theta_p^{t+1} - \theta\| \leq \alpha\|\theta_p^t - \theta\|, \qquad 0 < \alpha < 1. \tag{5}$$

*Hence $\|\theta_p^t - \theta\| \leq \alpha^t C_0$ with $C_0 = \|\theta_p^0 - \theta\|$.*

**Theorem 5.1.** *Under Assumptions 5.1 - 5.3, with probability at least $1 - \eta$,*

$$\left|\mathbb{E}_{(x,y)\in s_p} l(x, y; \theta) - \mathbb{E}_{(x,y)\sim D} l(x, y; \theta)\right| \;\leq\; \delta \;+\; 2L\,\alpha^t C_0. \tag{6}$$

*If $t = F_{\text{sync}}T$ synchronization cycles are executed over wall–clock time $T$, the bound becomes*

$$\delta + 2L\,C_0\,e^{-\lambda F_{\text{sync}}T}, \qquad \lambda = -\ln\alpha.$$

The discrepancy decomposes into (i) a *selection error* $\delta$ for the pruned proxy and (ii) a *mismatch* between selector and target that shrinks geometrically with the number/frequency of synchronizations. Hence, more frequent syncs (smaller $T_{\text{sync}}$) reduce the gap, matching our empirical curves. Detailed discussion and proof can be found in the Supplementary Materials.

## 6 Experiments

### 6.1 Experimental Setup

**Datasets.** The effectiveness of our approach is assessed on different image classification datasets: CIFAR-10 (Krizhevsky et al., 2009), CIFAR-100 (Krizhevsky et al., 2009), TinyImageNet-200 (Le & Yang, 2015), and ImageNet-1K (Deng et al., 2009). CIFAR-10 is partitioned into 50,000 training and 10,000 test samples, CIFAR-100 contains 100 classes and has 500 training and 100 testing samples per class, whereas TinyImageNet-200 contains 200 classes with 500 training, 50 validation, and 50 test samples per class. ImageNet-1K consists of 1,000 classes with approximately 1.2 million training images and 50,000 validation images, providing a comprehensive benchmark for evaluating large-scale image classification models. We also extend our experiments to text datasets (Amazon Review Polarity and Amazon Review Full) (Zhang & LeCun, 2015; Zhang et al., 2015) and to out-of-distribution (OOD) benchmark to assess generalization (results provided in Supplementary Materials 8.4).

**Implementation Details.** We used various model architectures: ResNet (ResNet-50, ResNet-56, ResNet-110, and ResNet-164), Wide-ResNet, VDCNN, and Vision Transformers (ViT) in our experiments. We pruned these architectures using the Torch-Pruning library (Fang et al., 2023) for different pruning ratios $p = 0.5, 0.6, 0.7$, and 0.8 to get the pruned architectures. We ran these experiments for 181 epochs following the setup in Coleman et al. (2020) for CIFAR-10 and CIFAR-100 and for 100 epochs for TinyImageNet-200 and ImageNet-1K. We used a mini-batch of 128 for CIFAR-10 and CIFAR-100 and 256 for TinyImageNet-200 and ImageNet-1K. Further details are provided in Supplementary Materials 8.3. We consider AL as a baseline for the proposed technique. Initially, we start by randomly selecting 2% of the data. For the first round, we add

Table 1: **Performance comparison** of Baseline and PruneFuse on CIFAR-10, CIFAR-100, Tiny ImageNet-200 and ImageNet-1K. This table summarizes the *top-1 test accuracy* of the final model (original in case of *AL* and Fused in *PruneFuse*) and *computational cost* of the data selector (in terms of FLOPs) for various pruning ratios ($p$) and labeling budgets($b$). *Params* corresponds to the number of parameters of the data selector model. All results use Least-Confidence sampling with $T_{\text{sync}} = 0$. ResNet-56 is utilized for CIFAR-10/100, while ResNet-50 is used for Tiny-ImageNet and ImageNet-1K. Results better than the Baseline are highlighted in **Bold**.

| | | ↑ **Accuracy (%)** | | | | | ↓ **Computation** ($\times 10^{16}$) | | | | |
|---|---|---|---|---|---|---|---|---|---|---|---|
| | ***Budget (b)*** | ***10%*** | ***20%*** | ***30%*** | ***40%*** | ***50%*** | ***10%*** | ***20%*** | ***30%*** | ***40%*** | ***50%*** |
| **Method** | **Params** | **CIFAR-10** | | | | | | | | | |
| Baseline (AL) | 0.85 M | 80.53±0.20 | 87.74±0.15 | 90.85±0.11 | 92.24±0.16 | 93.00±0.11 | 0.31 | 1.76 | 4.64 | 8.94 | 14.66 |
| PruneFuse $p$=0.5 | 0.21 M | **80.92±0.41** | **88.35±0.33** | **91.44±0.15** | **92.77±0.03** | **93.65±0.14** | **0.08** | **0.44** | **1.16** | **2.24** | **3.67** |
| PruneFuse $p$=0.6 | 0.14 M | **80.58±0.33** | **87.79±0.20** | **90.94±0.13** | **92.58±0.31** | **93.08±0.42** | **0.05** | **0.28** | **0.74** | **1.43** | **2.35** |
| PruneFuse $p$=0.7 | 0.08 M | 80.19±0.45 | **87.88±0.05** | 90.70±0.21 | **92.44±0.24** | **93.40±0.11** | **0.03** | **0.16** | **0.42** | **0.80** | **1.32** |
| PruneFuse $p$=0.8 | 0.03 M | 80.11±0.28 | 87.58±0.14 | 90.50±0.08 | **92.42±0.41** | **93.32±0.14** | **0.01** | **0.07** | **0.18** | **0.36** | **0.58** |
| **Method** | **Params** | **CIFAR-100** | | | | | | | | | |
| Baseline (AL) | 0.86 M | 35.99±0.80 | 52.99±0.56 | 59.29±0.46 | 63.68±0.53 | 66.72±0.33 | 0.31 | 1.77 | 4.67 | 9.00 | 14.76 |
| PruneFuse $p$=0.5 | 0.22 M | **40.26±0.95** | **53.90±1.06** | **60.80±0.44** | **64.98±0.40** | **67.87±0.17** | **0.08** | **0.44** | **1.17** | **2.26** | **3.70** |
| PruneFuse $p$=0.6 | 0.14 M | **37.82±0.83** | 52.65±0.40 | **60.08±0.22** | **63.70±0.25** | **66.89±0.46** | **0.05** | **0.28** | **0.75** | **1.44** | **2.36** |
| PruneFuse $p$=0.7 | 0.08 M | **36.76±0.63** | 52.15±0.53 | **59.33±0.17** | 63.65±0.36 | **66.84±0.43** | **0.03** | **0.16** | **0.42** | **0.81** | **1.34** |
| PruneFuse $p$=0.8 | 0.04 M | **36.49±0.20** | 50.98±0.54 | 58.53±0.50 | 62.87±0.13 | 65.85±0.32 | **0.01** | **0.07** | **0.19** | **0.37** | **0.60** |
| **Method** | **Params** | **Tiny-ImageNet-200** | | | | | | | | | |
| Baseline (AL) | 23.9 M | 14.86±0.11 | 33.62±0.52 | 43.96±0.22 | 49.86±0.56 | 54.65±0.38 | 0.50 | 2.73 | 7.11 | 13.64 | 22.32 |
| PruneFuse $p$=0.5 | 6.10 M | **18.71±0.21** | **39.70±0.31** | **47.41±0.20** | **51.84±0.10** | **55.89±1.21** | **0.13** | **0.70** | **1.81** | **3.48** | **5.69** |
| PruneFuse $p$=0.6 | 3.92 M | **19.25±0.72** | **38.84±0.70** | **47.02±0.30** | **52.09±0.29** | **55.29±0.28** | **0.08** | **0.45** | **1.16** | **2.23** | **3.66** |
| PruneFuse $p$=0.7 | 2.24 M | **18.32±0.95** | **39.24±0.75** | **46.45±0.58** | **52.02±0.65** | **55.63±0.55** | **0.05** | **0.26** | **0.67** | **1.28** | **2.09** |
| PruneFuse $p$=0.8 | 1.02 M | **18.34±0.93** | **37.86±0.42** | **47.15±0.31** | **51.77±0.40** | **55.18±0.50** | **0.02** | **0.12** | **0.30** | **0.58** | **0.95** |
| **Method** | **Params** | **ImageNet-1K** | | | | | | | | | |
| Baseline (AL) | 25.5 M | 52.97±0.20 | 64.52±0.46 | 69.30±0.15 | 71.98±0.11 | 73.56±0.16 | 6.88 | 37.34 | 97.28 | 186.70 | 305.60 |
| PruneFuse $p$=0.5 | 6.91 M | **55.03±0.33** | **65.12±0.31** | **69.72±0.17** | **72.07±0.28** | **73.86±0.55** | **1.86** | **10.10** | **26.30** | **50.47** | **82.62** |
| PruneFuse $p$=0.6 | 4.59 M | **54.69±0.93** | **65.13±0.55** | **69.74±0.38** | **72.48±0.33** | **74.00±0.68** | **1.24** | **6.71** | **17.47** | **33.53** | **54.88** |
| PruneFuse $p$=0.7 | 2.74 M | **53.73±0.71** | 64.43±0.65 | 68.95±0.41 | 71.81±0.31 | **73.84±0.29** | **0.74** | **4.00** | **10.43** | **20.01** | **32.76** |
| PruneFuse $p$=0.8 | 1.35 M | **53.08±0.22** | 64.00±0.17 | 69.00±0.90 | 71.79±0.81 | **73.64±0.52** | **0.36** | **1.97** | **5.14** | **9.86** | **16.14** |

8% from the unlabeled set, then 10% in each subsequent round, until the required budget $b$ is met. After each round, we retrain the models from scratch, as described in the methodology. All experiments were carried out independently three times, and the mean is reported. Detailed experiments on various model architectures, datasets, labeling budgets, and data selection metrics are provided in Supplementary Materials 8.4. We also provide detailed Complexity Analysis and Error Analysis for PruneFuse in Supplementary Materials 8.1 and 8.2, respectively.

### 6.2 Results and Discussions

**Main Experiments.** Table 1 benchmarks PruneFuse against the standard AL pipeline across different datasets. PruneFuse attains comparable or higher top-1 accuracy while consuming only a fraction of the computational resources measured in terms of FLOPs when computed for the whole training duration of the pruned network and the selection process for different label budgets. On CIFAR-10, with a pruned model ($p$=0.7), PruneFuse achieves similar or superior performance compared to the baseline, while reducing selector cost by more than 90% (e.g. 1.32 vs. 14.66 $\times 10^{16}$ FLOPs at $b$=50%). Similarly, on CIFAR-100 with ($p = 0.5$ at $b$=50%), PruneFuse outperforms baseline's accuracy by 1% while reducing 73% of the computational costs. The advantage becomes even more pronounced on the larger benchmarks. For Tiny-ImageNet, an aggressively pruned selector ($p$=0.8) lifts accuracy from 54.65% to 55.18% while reducing selector computation by 96%. Similarly, on ImageNet-1K, with the same pruning ratio, PruneFuse attains 73.64% (baseline 73.56%) yet requires 95% less computation. These results show that PruneFuse achieves a superior accuracy–cost trade-off compared to a typical AL pipeline.

We further investigated how the synchronization interval $T_{\text{sync}}$ shapes the accuracy–cost trade-off. Fig. 3 plots top-1 accuracy versus cumulative selector FLOPs for four pruning ratios using $T_{sync} = 0, 1$ (the pruned

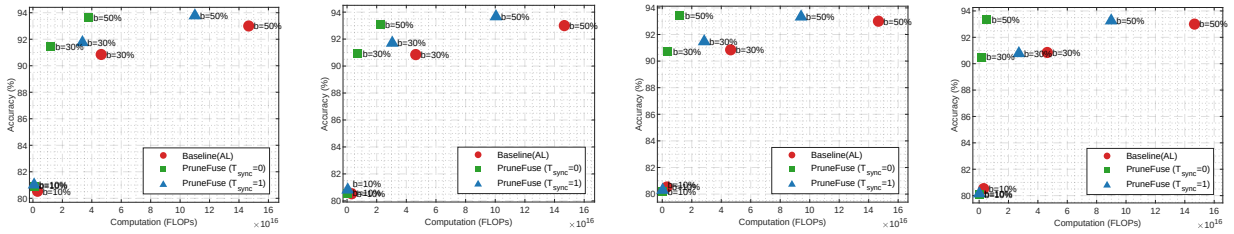


(a) $p = 0.5$ (b) $p = 0.6$ (c) $p = 0.7$ (d) $p = 0.8$

Figure 3: **Accuracy-cost trade-off** for PruneFuse. This figure illustrates the total number of FLOPs utilized by PruneFuse for data selection, compared to the baseline Active Learning method, for $T_{\text{sync}}$=0, 1 with labeling budgets $b = 10\%, 30\%, 50\%$. The experiments are conducted on the CIFAR-10 dataset using the ResNet-56 architecture. Subfigures (a), (b), (c), and (d) correspond to different pruning ratios of 0.5, 0.6, 0.7, and 0.8, respectively.

Table 2: **Comparison with baselines:** Final *top-1 test accuracy* and cumulative selector *cost* for different label budgets compared with baselines for ResNet-56 on CIFAR-10.

| **Method** | **Params** | **↑ Accuracy (%)** | | | | | **↓ Computation** ($\times 10^{16}$ FLOPs) | | | | |
|---|---|---|---|---|---|---|---|---|---|---|---|
| | *Budget (b)* | *10%* | *20%* | *30%* | *40%* | *50%* | *10%* | *20%* | *30%* | *40%* | 50% |
| Baseline (AL) | 0.85 M | 80.53±0.20 | 87.74±0.15 | 90.85±0.11 | 92.24±0.16 | 93.00±0.11 | 0.31 | 1.76 | 4.64 | 8.94 | 14.66 |
| SVP | 0.26 M | 80.76±0.70 | 87.31±0.56 | 90.77±0.45 | 92.59±0.25 | 92.95±0.33 | 0.10 | 0.56 | 1.47 | 2.84 | 4.66 |
| PruneFuse ($T_{\text{sync}}$=0) | 0.21 M | **80.92±0.41** | **88.35±0.33** | **91.44±0.15** | **92.77±0.03** | **93.65±0.14** | **0.08** | **0.44** | **1.16** | **2.24** | **3.67** |
| PruneFuse ($T_{\text{sync}}$=2) | 0.21 M | **80.90±0.21** | **88.40±0.46** | **91.55±0.63** | **93.05±0.36** | **93.74±0.44** | **0.08** | 1.17 | 1.89 | 5.14 | 6.58 |
| PruneFuse ($T_{\text{sync}}$=1) | 0.21 M | **81.02±0.46** | **88.52±0.37** | **91.76±0.08** | **93.15±0.18** | **93.78±0.45** | **0.08** | 1.17 | 3.34 | 6.60 | 10.94 |
| BALD | 0.85 M | 80.61±0.24 | 88.11±0.41 | 91.21±0.56 | 92.98±0.81 | 93.36±0.62 | 0.34 | 1.81 | 4.71 | 9.03 | 14.77 |
| PruneFuse ($T_{\text{sync}}$=1) + BALD | 0.21 M | **80.71±0.46** | **88.38±0.37** | **91.44±0.55** | **93.16±0.21** | **93.58±0.07** | **0.08** | **1.18** | **3.36** | **6.62** | **10.97** |
| ALSE | 0.85 M | 80.73±0.32 | 88.13±0.41 | 90.99±0.56 | 92.58±0.63 | 93.13±0.75 | 0.41 | 1.96 | 4.92 | 9.29 | 15.08 |
| PruneFuse ($T_{\text{sync}}$=0) + ALSE | 0.21 M | **80.80±0.51** | **88.17±0.35** | **91.43±0.45** | **93.02±0.55** | **93.19±0.61** | **0.10** | **0.49** | **1.23** | **2.32** | **3.70** |

selector is updated from the finetuned fused model after every AL round). In all cases, PruneFuse lies on a superior accuracy–cost curve compared with the AL baseline. Even the lightest variant ($p$=0.8) achieves baseline-level accuracy while spending only one-tenth of the computation, and the configuration with $T_{sync} = 1$ delivers the best overall trade-off.

**Comparison with Baselines.** Table 2 delineates a performance comparison of PruneFuse with several prominent works, including SVP, ALSE (Jung et al., 2023), and BALD. Here, SVP employs a ResNet-20 (0.26 M params) while PruneFuse uses a 50% pruned ResNet-56 (0.21 M params). ALSE utilizes 5 snapshots of the data selector model at various training steps for data selection. BALD, similar to baseline AL, uses ResNet-56 for data selection based on Bayesian uncertainty. Results demonstrate that PruneFuse consistently outperforms SVP across all label budgets. For example, PruneFuse peaks at 93.65% at $b$=50% compared to SVP with 92.95%, while having significantly lower computational costs (21% lower than SVP and 75% lower than the baseline). PruneFuse with iterative pruning of the fused model shows even better performance, reaching 93.78% and 93.74% accuracy with $T_{sync} = 1$ and 2 at 50% label budget, respectively, offering a trade-off between computational efficiency and accuracy. BALD demonstrates competitive results at higher label budgets (e.g., 93.36% at $b$=50%). However, BALD can be seamlessly integrated with PruneFuse. Capitalizing on the strengths of both methods, PruneFuse + BALD yields improved performance of 93.58% at 50% label budget while consuming 26% less computation. Similarly, PruneFuse + ALSE also results in better performance while having 4× less computation compared to ALSE.

Table 3 compares the performance of PruneFuse on the Coreset Selection task against various recent works. In this setup, the network is first trained on the entire dataset and then identifies a representative subset of data (coreset) based on the selection metric. The accuracy of the target model trained on that selected coreset is reported. The results show that PruneFuse seamlessly integrates with these advanced selection metrics, achieving competitive or superior performance compared to the baselines while being computationally inexpensive. This highlights the versatility of PruneFuse in enhancing existing coreset selection techniques.

**Additional Experiments and Ablation Studies.** Table 4 demonstrates results for Vision Transformers under multiple pruning ratios. We use a moderate sized ViT containing 21M parameters. Results show that

Table 3: **Evaluation on Coreset Selection task:** Baseline vs. PruneFuse ($p = 0.5$ and $T_{sync} = 0$) with Various Selection Metrics including Forgetting Events (Toneva et al., 2019), Moderate (Xia et al., 2023), and CSS (Zheng et al., 2023) on CIFAR-10 dataset using ResNet-56 architecture.

| Method | Model Params | | Budget ($b$) | Selection Metric | | | | |
|---|---|---|---|---|---|---|---|---|
| | Data Selector | Target Model | | Entropy | Least Conf. | Forgetting Events | Moderate | CSS |
| **Baseline** | 0.85M | 0.85M | 25% | 86.13±0.41 | 86.50±0.21 | 86.01±0.71 | 86.27±0.65 | 87.21±0.68 |
| **PruneFuse** | 0.21M | 0.85M | | **86.71±0.44** | **86.68±0.42** | **87.84±0.09** | **87.63±0.31** | **88.85±0.29** |
| **Baseline** | 0.85M | 0.85M | 50% | 91.41±0.21 | 91.28±0.35 | 93.31±0.76 | 90.97±0.55 | 90.68±0.35 |
| **PruneFuse** | 0.21M | 0.85M | | **92.24±0.45** | **92.75±0.65** | **93.40±0.19** | **91.08±0.49** | **90.79±0.51** |

Table 4: **Performance Comparison** of Baseline and PruneFuse on CIFAR-10 and CIFAR-100 with **Vision Transformers (ViT)**. This table summarizes the test accuracy of final models (original in case of AL and Fused in PruneFuse) for various pruning ratios ($p$) and labeling budgets ($b$).

| Method | CIFAR-10 | | | | | CIFAR-100 | | | | |
|---|---|---|---|---|---|---|---|---|---|---|
| | Label Budget ($b$) | | | | | Label Budget ($b$) | | | | |
| | **10%** | **20%** | **30%** | **40%** | **50%** | **10%** | **20%** | **30%** | **40%** | **50%** |
| Baseline ($AL$) | 53.63 | 65.62 | 71.09 | 76.86 | 80.59 | 36.59 | 52.19 | 58.59 | 63.8 | 64.02 |
| PruneFuse ($p = 0.5$) | **59.32** | **71.63** | **75.61** | **81.50** | **83.64** | **46.84** | **57.16** | **62.56** | **65.8** | **67.75** |
| PruneFuse ($p = 0.6$) | **57.80** | **70.45** | **75.22** | **80.22** | **82.77** | **45.60** | **56.04** | **61.09** | **65.01** | **67.24** |
| PruneFuse ($p = 0.7$) | **56.17** | **69.25** | **73.87** | **79.47** | **82.15** | **44.46** | **55.36** | **60.99** | **64.47** | **66.85** |

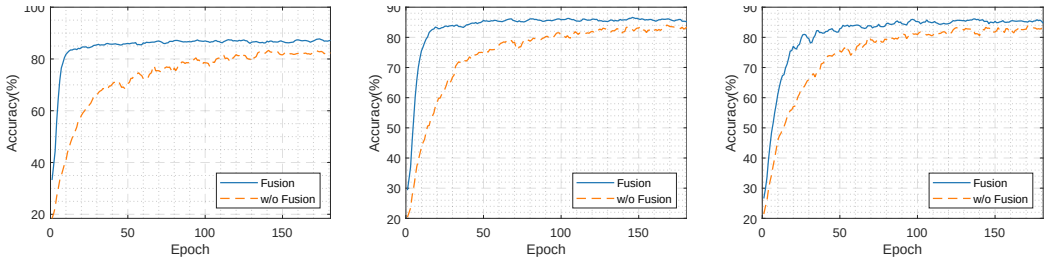


(a) $p = 0.5$ (b) $p = 0.6$ (c) $p = 0.7$

Figure 4: **Impact of Model Fusion on PruneFuse performance:** This figure compares the accuracy over epochs between fused and non-fused training approaches within the PruneFuse framework using ResNet-56 on CIFAR-10. Subfigures (a), (b), and (c) correspond to $p = 0.5$, 0.6, and 0.7, respectively, for $b = 30\%$.

PruneFuse consistently outperforms the standard AL baseline across all label budgets for both CIFAR-10 and CIFAR-100 datasets despite operating with substantially smaller selector models. On CIFAR-10, PruneFuse with $p$=0.5 yields strong gains at low budgets (e.g., +5.69 points at $b$=10%) and maintains improvements even at higher budgets (e.g., +3.05 points at $b$=50%). The gains are even more pronounced on CIFAR-100, where the same configuration improves performance by +10.25 points at $b$=10% and offers consistent 3–4 point improvements at larger budgets. Notably, the advantages persist even under aggressive pruning. With $p$=0.7, PruneFuse remains superior to the unpruned baseline across all label budgets (e.g., 56.17% vs. 53.63% on CIFAR-10 and 44.46% vs. 36.59% on CIFAR-100 at $b$=10%).

We also extend our evaluation beyond vision tasks. Table 5 delineates experiments on text classification using VDCNN for Amazon Review Polarity and Amazon Review Full. PruneFuse again improves on the AL baseline in all pruning ratios and label budgets. In the case of Amazon Review Polarity, PruneFuse delivers consistent gains (e.g., 94.13 → 94.66% at $b$=10%, and 95.71 → 95.87% at $b$=50%). On the other hand, the improvements are greater for the Amazon Full dataset: with $p$=0.5, PruneFuse improves the baseline by 0.8–1.0 points across all budgets, and even with $p$=0.8 it continues to match or surpass the unpruned model. A consistent trend across both datasets is the stability of performance across pruning ratios ($p$=0.5–0.8). These observations highlight the robustness of PruneFuse, indicating the effectiveness of heavily pruned selectors in data selection while being substantially computationally efficient.

Table 5: **Performance comparison** of Baseline and PruneFuse on Amazon Review Polarity Dataset and Amazon Review Full Dataset with VDCNN Architecture. This table summarizes the test accuracy of final models (original in case of AL and Fused in PruneFuse) for various pruning ratios ($p$) and labeling budgets ($b$).

| Method | Amazon Review Polarity | | | | | Amazon Review Full | | | | |
|---|---|---|---|---|---|---|---|---|---|---|
| | Label Budget ($b$) | | | | | Label Budget ($b$) | | | | |
| | **10%** | **20%** | **30%** | **40%** | **50%** | **10%** | **20%** | **30%** | **40%** | **50%** |
| Baseline ($AL$) | 94.13 | 95.06 | 95.54 | 95.73 | 95.71 | 58.46 | 60.65 | 61.50 | 62.20 | 62.43 |
| PruneFuse ($p = 0.5$) | **94.66** | **95.45** | **95.71** | **95.87** | **95.87** | **59.45** | **61.28** | **62.02** | **62.66** | **62.84** |
| PruneFuse ($p = 0.6$) | **94.62** | **95.38** | **95.69** | **95.82** | **95.88** | **59.28** | **61.14** | **62.08** | **62.62** | **62.81** |
| PruneFuse ($p = 0.7$) | **94.47** | **95.43** | **95.71** | **95.83** | **95.84** | **59.42** | **61.05** | **61.98** | **62.48** | **62.85** |
| PruneFuse ($p = 0.8$) | **94.33** | **95.37** | **95.63** | **95.79** | **95.85** | **59.24** | **61.05** | **61.94** | **62.45** | **62.77** |

Table 6: **Effect of Pruning techniques and Pruning criteria** on PruneFuse ($p = 0.5$) on CIFAR-10 dataset with ResNet-56.

| Method | Pruning Technique | Pruning Criteria | Label Budget ($b$) | | | | |
|---|---|---|---|---|---|---|---|
| | | | **10%** | **20%** | **30%** | **40%** | **50%** |
| **Baseline (AL)** | - | - | 80.53 | 87.74 | 90.85 | 92.24 | 93.00 |
| **PruneFuse** ($T_{sync} = 0$) | Dynamic Pruning | Magnitude Imp. | 79.73 | 87.16 | **91.08** | **92.29** | **93.19** |
| | | GroupNorm Imp. | 80.10 | **88.25** | **91.01** | **92.25** | **93.74** |
| | | LAMP Imp. | **81.51** | 87.45 | 90.64 | **92.41** | **93.25** |
| **PruneFuse** ($T_{sync} = 0$) | Static Pruning | Magnitude Imp. | **80.92** | **88.35** | **91.44** | **92.77** | **93.65** |
| | | GroupNorm Imp. | **80.84** | **88.20** | **91.19** | **93.01** | **93.03** |
| | | LAMP Imp. | **81.10** | **88.37** | **91.32** | **93.02** | **93.08** |
| **PruneFuse** ($T_{sync} = 1$) | Static Pruning | Magnitude Imp. | **81.23** | **88.52** | **91.76** | **93.15** | **93.78** |
| | | GroupNorm Imp. | **81.09** | **88.77** | **91.77** | **93.19** | **93.68** |
| | | LAMP Imp. | **81.86** | **88.51** | **92.10** | **93.02** | **93.63** |

Fig. 4 demonstrates the effect of fusion across various pruning ratios; the models trained with fusion in-place perform better than those trained without fusion, achieving higher accuracy levels at an accelerated pace. The rapid convergence is most notable in the initial training phases, where the fused model benefits from the initialization provided by integrating weights from a trained pruned model $\theta_p^*$ with an untrained model $\theta$. The strategic retention of untrained weights introduces a beneficial stochastic component to the training process, enhancing the model's ability to explore new regions of the parameter space. This dual capability of exploiting prior knowledge and exploring new configurations enables the proposed technique to consistently outperform, making it particularly beneficial in scenarios with sparse label data.

In Table 6, we evaluate the impact of different pruning techniques (e.g., static pruning, dynamic pruning) and pruning criteria (e.g., L2 norm, GroupNorm Importance, LAMP Importance Fang et al. (2023)) on the performance of PruneFuse. Static pruning involves pruning the entire network at once at the start of training, whereas dynamic pruning incrementally prunes the network in multiple steps during training. In our implementation of dynamic pruning, the network is pruned in five steps over the course of 20 epochs. The results demonstrate that PruneFuse is highly adaptable to various pruning strategies, consistently maintaining strong performance in data selection tasks. This flexibility underscores the robustness of the framework across different pruning approaches and criteria.

## 7 Conclusion

In this work, we present PruneFuse, a novel strategy that integrates pruning with network fusion to optimize the data selection pipeline for deep learning. PruneFuse leverages a small pruned model for data selection, which then seamlessly fuses with the original model, providing faster training, better generalization, and significantly reduced computational costs. It consistently outperforms existing baselines while offering a scalable, practical, and flexible solution in resource-constrained settings.

## References


Cody Coleman, Christopher Yeh, Stephen Mussmann, Baharan Mirzasoleiman, Peter Bailis, Percy Liang, Jure Leskovec, and Matei Zaharia. Selection via proxy: Efficient data selection for deep learning. *The Eighth International Conference on Learning Representations*, 2020.

J. Deng, W. Dong, R. Socher, L.-J. Li, K. Li, and L. Fei-Fei. ImageNet: A Large-Scale Hierarchical Image Database. In *CVPR09*, 2009.

Xiaohan Ding, Guiguang Ding, Yuchen Guo, and Jungong Han. Centripetal sgd for pruning very deep convolutional networks with complicated structure. In *Proceedings of the IEEE/CVF conference on computer vision and pattern recognition*, pp. 4943–4953, 2019.

Xin Dong, Shangyu Chen, and Sinno Pan. Learning to prune deep neural networks via layer-wise optimal brain surgeon. *Advances in neural information processing systems*, 30, 2017.

Zhen Dong, Zhewei Yao, Daiyaan Arfeen, Amir Gholami, Michael W Mahoney, and Kurt Keutzer. Hawq-v2: Hessian aware trace-weighted quantization of neural networks. *Advances in neural information processing systems*, 33:18518–18529, 2020.

Gongfan Fang, Xinyin Ma, Mingli Song, Michael Bi Mi, and Xinchao Wang. Depgraph: Towards any structural pruning. In *Proceedings of the IEEE/CVF Conference on Computer Vision and Pattern Recognition*, pp. 16091–16101, 2023.

Jonathan Frankle, Gintare Karolina Dziugaite, Daniel M Roy, and Michael Carbin. Pruning neural networks at initialization: Why are we missing the mark? *The Ninth International Conference on Learning Representations*, 2021.

Alexander Freytag, Erik Rodner, and Joachim Denzler. Selecting influential examples: Active learning with expected model output changes. In *Computer Vision–ECCV 2014: 13th European Conference, Zurich, Switzerland, September 6-12, 2014, Proceedings, Part IV 13*, pp. 562–577. Springer, 2014.

Yarin Gal, Riashat Islam, and Zoubin Ghahramani. Deep bayesian active learning with image data. In *Proceedings of the 34th International Conference on Machine Learning-Volume 70*, pp. 1183–1192. JMLR. org, 2017.

Trevor Gale, Erich Elsen, and Sara Hooker. The state of sparsity in deep neural networks. *arXiv preprint arXiv:1902.09574*, 2019.

Yiwen Guo, Anbang Yao, and Yurong Chen. Dynamic network surgery for efficient dnns. *Advances in neural information processing systems*, 29, 2016.

Song Han, Huizi Mao, and William J Dally. Deep compression: Compressing deep neural networks with pruning, trained quantization and huffman coding. *The forth International Conference on Learning Representations*, 2016.

Kaiming He, Xiangyu Zhang, Shaoqing Ren, and Jian Sun. Deep residual learning for image recognition. In *Proceedings of the IEEE conference on computer vision and pattern recognition*, pp. 770–778, 2016.

Yihui He, Xiangyu Zhang, and Jian Sun. Channel pruning for accelerating very deep neural networks. In *Proceedings of the IEEE international conference on computer vision*, 2017.

Geoffrey Hinton, Oriol Vinyals, and Jeff Dean. Distilling the knowledge in a neural network. *arXiv preprint arXiv:1503.02531*, 2015.

Benoit Jacob, Skirmantas Kligys, Bo Chen, Menglong Zhu, Matthew Tang, Andrew Howard, Hartwig Adam, and Dmitry Kalenichenko. Quantization and training of neural networks for efficient integer-arithmetic-only inference. In *Proceedings of the IEEE conference on computer vision and pattern recognition*, pp. 2704–2713, 2018.

Eeshaan Jain, Tushar Nandy, Gaurav Aggarwal, Ashish Tendulkar, Rishabh Iyer, and Abir De. Efficient data subset selection to generalize training across models: Transductive and inductive networks. *Advances in Neural Information Processing Systems*, 36, 2023.

Seohyeon Jung, Sanghyun Kim, and Juho Lee. A simple yet powerful deep active learning with snapshots ensembles. In *The Eleventh International Conference on Learning Representations*, 2023.

Christoph Käding, Erik Rodner, Alexander Freytag, and Joachim Denzler. Active and continuous exploration with deep neural networks and expected model output changes. *arXiv preprint arXiv:1612.06129*, 2016.

Krishnateja Killamsetty, Sivasubramanian Durga, Ganesh Ramakrishnan, Abir De, and Rishabh Iyer. Grad-match: Gradient matching based data subset selection for efficient deep model training. In *International Conference on Machine Learning*, pp. 5464–5474. PMLR, 2021a.

Krishnateja Killamsetty, Durga Subramanian, Ganesh Ramakrishnan, and Rishabh Iyer. Glister: A generalization based data selection framework for efficient and robust learning. AAAI, 2021b.

Andreas Kirsch, Joost Van Amersfoort, and Yarin Gal. Batchbald: Efficient and diverse batch acquisition for deep bayesian active learning. *Advances in neural information processing systems*, 32, 2019.

Alex Krizhevsky, Geoffrey Hinton, et al. Learning multiple layers of features from tiny images. 2009.

Ya Le and Xuan Yang. Tiny imagenet visual recognition challenge. *CS 231N*, 7(7):3, 2015.

Namhoon Lee, Thalaiyasingam Ajanthan, and Philip HS Torr. Snip: Single-shot network pruning based on connection sensitivity. *The Seventh International Conference on Learning Representations*, 2019.

Hao Li, Asim Kadav, Igor Durdanovic, Hanan Samet, and Hans Peter Graf. Pruning filters for efficient convnets. *arXiv preprint arXiv:1608.08710*, 2016.

Zhuang Liu, Jianguo Li, Zhiqiang Shen, Gao Huang, Shoumeng Yan, and Changshui Zhang. Learning efficient convolutional networks through network slimming. In *Proceedings of the IEEE international conference on computer vision*, pp. 2736–2744, 2017.

Jonathan Long, Evan Shelhamer, and Trevor Darrell. Fully convolutional networks for semantic segmentation. In *Proceedings of the IEEE conference on computer vision and pattern recognition*, pp. 3431–3440, 2015.

Jongsoo Park, Sheng Li, Wei Wen, Ping Tak Peter Tang, Hai Li, Yiran Chen, and Pradeep Dubey. Faster cnns with direct sparse convolutions and guided pruning. *The Fifth International Conference on Learning Representations*, 2017.

Sejun Park, Jaeho Lee, Sangwoo Mo, and Jinwoo Shin. Lookahead: A far-sighted alternative of magnitude-based pruning. *The Eighth International Conference on Learning Representations*, 2020.

Shaoqing Ren, Kaiming He, Ross Girshick, and Jian Sun. Faster r-cnn: Towards real-time object detection with region proposal networks. *Advances in neural information processing systems*, 28, 2015.

Alex Renda, Jonathan Frankle, and Michael Carbin. Comparing rewinding and fine-tuning in neural network pruning. *The Eighth International Conference on Learning Representations*, 2020.

Ozan Sener and Silvio Savarese. Active learning for convolutional neural networks: A core-set approach. *The Sixth International Conference on Learning Representations*, 2018a.

Ozan Sener and Silvio Savarese. Active learning for convolutional neural networks: A core-set approach. In *International Conference on Learning Representations*, 2018b.

Burr Settles. Active learning. *Synthesis Lectures on Artificial Intelligence and Machine Learning*, 6(1):1–114, 2012.

Claude Elwood Shannon. A mathematical theory of communication. *The Bell system technical journal*, 27 (3):379–423, 1948.

Yanyao Shen, Hyokun Yun, Zachary Lipton, Yakov Kronrod, and Animashree Anandkumar. Deep active learning for named entity recognition. In *Proceedings of the 2nd Workshop on Representation Learning for NLP*. Association for Computational Linguistics, 2018.

Chen Sun, Abhinav Shrivastava, Saurabh Singh, and Abhinav Gupta. Revisiting unreasonable effectiveness of data in deep learning era. In *Proceedings of the IEEE international conference on computer vision*, pp. 843–852, 2017.

Hidenori Tanaka, Daniel Kunin, Daniel L Yamins, and Surya Ganguli. Pruning neural networks without any data by iteratively conserving synaptic flow. *Advances in neural information processing systems*, 33: 6377–6389, 2020.

Mariya Toneva, Alessandro Sordoni, Remi Tachet des Combes, Adam Trischler, Yoshua Bengio, and Geoffrey J Gordon. An empirical study of example forgetting during deep neural network learning. *arXiv preprint arXiv:1812.05159*, 2019.

Joost van Amersfoort, Milad Alizadeh, Sebastian Farquhar, Nicholas Lane, and Yarin Gal. Single shot structured pruning before training. *arXiv preprint arXiv:2007.00389*, 2020.

Alvin Wan, Xiaoliang Dai, Peizhao Zhang, Zijian He, Yuandong Tian, Saining Xie, Bichen Wu, Matthew Yu, Tao Xu, Kan Chen, et al. Fbnetv2: Differentiable neural architecture search for spatial and channel dimensions. In *Proceedings of the IEEE/CVF conference on computer vision and pattern recognition*, 2020.

Yulong Wang, Xiaolu Zhang, Lingxi Xie, Jun Zhou, Hang Su, Bo Zhang, and Xiaolin Hu. Pruning from scratch. In *Proceedings of the AAAI Conference on Artificial Intelligence*, volume 34, pp. 12273–12280, 2020.

Xiaobo Xia, Jiale Liu, Jun Yu, Xu Shen, Bo Han, and Tongliang Liu. Moderate coreset: A universal method of data selection for real-world data-efficient deep learning. In *The Eleventh International Conference on Learning Representations*, 2023.

Sang Michael Xie, Shibani Santurkar, Tengyu Ma, and Percy S Liang. Data selection for language models via importance resampling. *Advances in Neural Information Processing Systems*, 36:34201–34227, 2023.

Hongxu Yin, Pavlo Molchanov, Jose M Alvarez, Zhizhong Li, Arun Mallya, Derek Hoiem, Niraj K Jha, and Jan Kautz. Dreaming to distill: Data-free knowledge transfer via deepinversion. In *Proceedings of the IEEE/CVF Conference on Computer Vision and Pattern Recognition*, pp. 8715–8724, 2020.

Zhonghui You, Kun Yan, Jinmian Ye, Meng Ma, and Ping Wang. Gate decorator: Global filter pruning method for accelerating deep convolutional neural networks. *Advances in neural information processing systems*, 32, 2019.

Yang Yu, Kai Han, Hang Zhou, Yehui Tang, Kaiqi Huang, Yunhe Wang, and Dacheng Tao. LLM data selection and utilization via dynamic bi-level optimization. In *Forty-second International Conference on Machine Learning*, 2025.

Zichun Yu, Spandan Das, and Chenyan Xiong. Mates: Model-aware data selection for efficient pretraining with data influence models. *Advances in Neural Information Processing Systems*, 37:108735–108759, 2024.

Xiang Zhang and Yann LeCun. Text understanding from scratch. *arXiv preprint arXiv:1502.01710*, 2015.

Xiang Zhang, Junbo Zhao, and Yann LeCun. Character-level convolutional networks for text classification. *Advances in neural information processing systems*, 28, 2015.

Haizhong Zheng, Rui Liu, Fan Lai, and Atul Prakash. Coverage-centric coreset selection for high pruning rates. *arXiv preprint arXiv:2210.15809*, 2023.

Shuchang Zhou, Yuxin Wu, Zekun Ni, Xinyu Zhou, He Wen, and Yuheng Zou. Dorefa-net: Training low bitwidth convolutional neural networks with low bitwidth gradients. *arXiv preprint arXiv:1606.06160*, 2016.

Michael Zhu and Suyog Gupta. To prune, or not to prune: exploring the efficacy of pruning for model compression. *arXiv preprint arXiv:1710.01878*, 2017.

Barret Zoph and Quoc V Le. Neural architecture search with reinforcement learning. *arXiv preprint arXiv:1611.01578*, 2016.

# 8 Supplementary Materials

This Supplementary Material provides additional details, analyses, and results to complement the main paper. The content is organized into the following subsections:

1. **Complexity Analysis** (8.1): A detailed breakdown of the computational complexity of PruneFuse and its components.
2. **Error Analysis for PruneFuse** (8.2): An error analysis outlining theoretical guarantees for the proposed framework.
3. **Implementation Details** (8.3): Specific details about the experimental setup, hyperparameters, and configurations used in our experiments.
4. **Performance Comparison with Different Datasets, Selection Metrics, and Architectures** (8.4): Results demonstrating PruneFuse's adaptability across datasets and architectures.
5. **Ablation Study of Fusion** (8.5): Analysis of the impact of the fusion process on PruneFuse's performance.
6. **Ablation Study of Knowledge Distillation in PruneFuse** (8.6): An evaluation of the role of knowledge distillation in improving performance.
7. **Comparison with SVP** (8.7): A comparison highlighting differences and improvements over the SVP baseline.
8. **Ablation Study on the Number of Selected Data Points ($k$)** (8.8): Investigation of how varying $k$ affects PruneFuse's performance.
9. **Impact of Early Stopping on Performance** (8.9): Evaluation of the utility of early stopping when integrated with PruneFuse.
10. **Performance Comparison Across Architectures and Datasets** (8.10): Additional results comparing PruneFuse's performance on various architectures and datasets.
11. **Performance at Lower Pruning Rates** (8.11): Results demonstrating PruneFuse's effectiveness at lower pruning rates.
12. **Comparison with Recent Coreset Selection Techniques** (8.12): Evaluation of PruneFuse's performance with recent coreset selection methods.
13. **Effect of Various Pruning Strategies and Criteria** (8.13): Analysis of different pruning techniques and criteria on PruneFuse's performance.
14. **Detailed Runtime Analysis of PruneFuse** (8.14): A detailed runtime analysis of PruneFuse compared to baseline methods.

Each section provides additional insights, evaluations, and experiments to further validate and explain the effectiveness of the proposed approach.

### 8.1 Complexity Analysis

Given $P$ and $N$ represent the total number of parameters in the pruned and dense model, where $P \ll N$, the computational costs can be summarized as follows:

**Initial Training on $s_0$:**

$$\begin{aligned} \text{PruneFuse:} \quad & O\left(|s_0| \times P \times T\right) + O\left(P \times \log P\right) \text{ one time pruning cost} \\ \text{Baseline AL:} \quad & O\left(|s_0| \times N \times T\right) \end{aligned}$$

**Data selection round with current labeled pool L:**

$$\begin{aligned} \text{PruneFuse:} \quad & O\left(|L| \times P \times T\right) + O\left(|U| \times P\right) \text{ selection} \\ \text{Baseline AL:} \quad & O\left(|L| \times N \times T\right) + O\left(|U| \times N\right) \text{ selection} \end{aligned}$$

**Training of the final model on the final labeled set L:**

$$\begin{aligned} \text{PruneFuse:} \quad & O\left(|L| \times N \times T\right) + O\left(P\right) \text{ one time fusion cost} \\ \text{Baseline AL:} \quad & O\left(|L| \times N \times T\right) \end{aligned}$$

**Total training complexity:**

$$\begin{aligned} \text{PruneFuse:} \quad & O\left(|s_0| \times P \times T\right) + O\left(P \times \log P\right) + R \times \left[O\left(|L| \times P \times T\right) + O\left(|U| \times P\right)\right] \\ & + F_{sync} * \left[O\left(|L| \times N \times T\right) + O(P) + O\left(|L| \times P \times T\right) + O\left(P \times \log P\right)\right] \\ & + O\left(|L| \times N \times T\right) + O(P) \\ \text{Baseline AL:} \quad & O\left(|s_0| \times N \times T\right) + R \times \left[O\left(|L| \times N \times T\right) + O\left(|U| \times N\right)\right] + O\left(|L| \times N \times T\right) \end{aligned}$$

Here $T$ represents the total number of epochs for a training round of AL which in our case is set to 181. $U$ is the whole unlabeled dataset and $R$ represents the total number of AL rounds. $F_{sync}$ represents the frequency of iterative pruning based on the fused model.

We can see that the major training costs in Active Learning (AL) arise from the repeated use of a large, dense model, which significantly increases computational expenses, especially across multiple rounds of data selection. By using a smaller surrogate (pruned model) for these rounds, as implemented in PruneFuse, the training cost and overall computation are reduced substantially. This approach leads to a more efficient and cost-effective data selection process, allowing for better resource utilization while maintaining high performance.

### 8.2 Error Bound for PruneFuse

Let $\theta$ denote the full network trained on the entire distribution $D$ and $\mathbb{E}_{(x,y)\sim D}\big[l(x,y;\theta)\big]$ be its population loss. After $t$ *prune–select–fuse* cycles, PruneFuse holds a pruned selector $\theta_p^t$ and the subset it selected, $s_p \subset D$. We analyze

$$\big|\mathbb{E}_{(x,y)\in s_p} l(x,y;\theta) - \mathbb{E}_{(x,y)\sim D} l(x,y;\theta)\big|, \tag{7}$$

i.e. the error incurred by training the *full* model on the selected subset instead of whole $D$.

**Assumption 1.** *The loss function $l(x,y;\theta)$ is Lipschitz continuous with respect to the model parameters $\theta$, with constant $L$:*

$$|l(x,y;\theta_1) - l(x,y;\theta_2)| \le L\|\theta_1 - \theta_2\| \tag{8}$$

**Assumption 2.** *The pruned subset $s_p$ is selected using the pruned model $\theta_p$ using an acquisition score (e.g. Least Confidence or Entropy), and the expected loss over $s_p$ approximates that over $D$ with probability at least $1-\eta$ (over the randomness of the selection rule). Specifically,*

$$\big|\mathbb{E}_{(x,y)\in s_p}[l(x,y;\theta_p)] - \mathbb{E}_{(x,y)\in D}[l(x,y;\theta_p)]\big| \le \delta \tag{9}$$

*Thus the subset yields a $\delta$–accurate estimate of the population loss.*

**Assumption 3.** *After each synchronization step, the pruned model $\theta_p$ is derived from the full model $\theta$. Specifically, each fusion step contracts the gap by a factor $\alpha$:*

$$\|\theta_p^{t+1} - \theta\| \leq \alpha \|\theta_p^t - \theta\|, \qquad 0 < \alpha < 1. \tag{10}$$

*Hence $\|\theta_p^t - \theta\| \leq \alpha^t C_0$ with $C_0 = \|\theta_p^0 - \theta\|$.*

**Theorem 8.1.** *Under Assumptions A1 - A3, with probability at least $1 - \eta$,*

$$\left| \mathbb{E}_{(x,y)\in s_p} l(x, y; \theta) - \mathbb{E}_{(x,y)\sim D} l(x, y; \theta) \right| \;\leq\; \delta \;+\; 2L\, \alpha^{\,t} C_0. \tag{11}$$

*If $t = F_{\text{sync}} T$ synchronization cycles are executed over wall–clock time $T$, the bound becomes*

$$\delta + 2L\, C_0\, e^{-\lambda F_{\text{sync}} T}, \qquad \lambda = -\ln \alpha.$$

**Proof.** By the triangle inequality,

$$\begin{aligned}
&\left| \mathbb{E}_{(x,y)\in s_p} l(x, y; \theta) - \mathbb{E}_{(x,y)\sim D} l(x, y; \theta) \right| \\
&\leq \left| \mathbb{E}_{(x,y)\in s_p} l(x, y; \theta) - \mathbb{E}_{(x,y)\in s_p} l(x, y; \theta_p^t) \right| \\
&\quad + \left| \mathbb{E}_{(x,y)\in s_p} l(x, y; \theta_p^t) - \mathbb{E}_{(x,y)\sim D} l(x, y; \theta_p^t) \right| \\
&\quad + \left| \mathbb{E}_{(x,y)\sim D} l(x, y; \theta_p^t) - \mathbb{E}_{(x,y)\sim D} l(x, y; \theta) \right|.
\end{aligned}$$

The middle term is bounded by $\delta$ with probability at least $1-\eta$ by Assumption 2. By Assumption 1 (Lipschitz continuity of the loss), the first and third terms are each at most $L\|\theta - \theta_p^t\|$. Therefore, with probability at least $1 - \eta$,

$$\begin{aligned}
&\left| \mathbb{E}_{(x,y)\in s_p} l(x, y; \theta) - \mathbb{E}_{(x,y)\sim D} l(x, y; \theta) \right| \\
&\quad \leq L\|\theta - \theta_p^t\| + \delta + L\|\theta - \theta_p^t\| \\
&\quad = \delta + 2L\|\theta - \theta_p^t\| \\
&\quad \leq \delta + 2L\alpha^t C_0,
\end{aligned}$$

where the last inequality follows from repeated application of Assumption 3, which gives $\|\theta - \theta_p\| \leq \alpha^t C_0$. The exponential form in the theorem statement follows immediately from $\alpha^t = e^{-\lambda t}$ with $\lambda = -\ln \alpha$.

For the $F_{\text{sync}}$=0 case with no fusion, the bound remains $\delta + 2L\, C_0$. Here, $\delta$ is the intrinsic error of using the informative subset instead of the full distribution. The extra term $L\, \alpha^t C_0$ measures how far the selector $\theta_p$ has drifted from the full model $\theta$; it decays geometrically with every fusion step. Thus, a modest synchronization frequency drives the total discrepancy to the $\delta$ floor (same as that of typical Active Learning) while keeping the whole data selection efficient.

### 8.3 Implementation Details.

We used ResNet-50, ResNet-56, ResNet-110, ResNet-164, Wide-ResNet, VDCNN, and Vision transformers architectures in our experiments. We pruned these architectures using the Torch-Pruning library (Fang et al., 2023) for different pruning ratios $p = 0.5, 0.6, 0.7$, and 0.8 to get the pruned architectures. For CIFAR-10 and CIFAR-100, the models were trained for 181 epochs, with an epoch schedule of [1, 90, 45, 45], and corresponding learning rates of [0.01, 0.1, 0.01, 0.001], using a momentum of 0.9 and weight decay of 0.0005. For TinyImageNet-200 and ImageNet-1K, the models were trained over an epoch schedule of [1, 1, 1, 1, 1, 25, 30, 20, 20], with learning rates of [0.0167, 0.0333, 0.05, 0.0667, 0.0833, 0.1, 0.01, 0.001, 0.0001], a momentum of 0.9, and weight decay of 0.0001. We use the mini-batch of 128 for CIFAR-10 and CIFAR-100 and 256 for

TinyImageNet-200 and ImageNet-1K. We also extend our experiments to text datasets: Amazon Review Polarity and Full (Zhang & LeCun, 2015; Zhang et al., 2015). Amazon Review Polarity has 3.6 million reviews split evenly between positive and negative ratings, with an additional 400,000 reviews for testing. Amazon Review Full has 3 million reviews split evenly between the 5 stars with an additional 650,000 reviews for testing. For Amazon Review Polarity and Full, the models were trained over an epoch schedule of [3, 3, 3, 3, 3], with learning rates of [0.01, 0.005, 0.0025, 0.00125, 0.000625], a momentum of 0.9, weight decay of 0.0001, and a mini-batch size of 128. For all the experiments SGD is used as an optimizer. We set the knowledge distillation coefficient $\lambda$ to 0.3. We took Active Learning (AL) as a baseline for the proposed technique and initially, we started by randomly selecting 2% of the data. For the first round, we added 8% from the unlabeled set, then 10% in each subsequent round, until reaching the label budget, $b$. After each round, we retrained the models from scratch, as described in the methodology. All experiments are carried out independently 3 times and then the average is reported.

### 8.4 Performance Comparison with different Datasets, Selection Metrics, and Architectures

To comprehensively evaluate the effectiveness of PruneFuse, we conducted additional experiments comparing its performance with baseline utilizing other data selection metrics such as Least Confidence, Entropy, and Greedy k-centers. Results are shown in Tables 7, 8, 9 and 10 for various architectures and labeling budgets. In all cases, our results demonstrate that PruneFuse mostly outperforms the baseline using these traditional metrics across various datasets and model architectures, highlighting the robustness of PruneFuse in selecting the most informative samples efficiently.

We further performed experiments on ViT, MobileNet for Vision task in Table 11, 12 and VDCNN for NLP tasks in Table 13, 14, to underscore PruneFuse's consistent efficiency and robust accuracy across different architectures and domains. Moreover, we demonstrated that PruneFuse does not degrade performance on OOD datasets in Table 15, reinforcing PruneFuse's stability.

Table 7: **Performance Comparison** of Baseline and PruneFuse on CIFAR-10 and CIFAR-100 with ResNet-56 architecture. This table summarizes the test accuracy of final models (original in case of AL and Fused in PruneFuse) for various pruning ratios ($p$), labeling budgets ($b$), and data selection metrics.

| **Method** | **Selection Metric** | **Label Budget ($b$)** | | | | |
|---|---|---|---|---|---|---|
| | | **10%** | **20%** | **30%** | **40%** | **50%** |
| Baseline *AL* | Least Conf | 80.53 ± 0.20 | 87.74 ± 0.15 | 90.85 ± 0.11 | 92.24 ± 0.16 | 93.00 ± 0.11 |
| | Entropy | 80.14 ± 0.41 | 87.63 ± 0.10 | 90.80 ± 0.36 | 92.51 ± 0.34 | 92.98 ± 0.03 |
| | Random | 78.55 ± 0.38 | 85.26 ± 0.21 | 88.13 ± 0.35 | 89.81 ± 0.15 | 91.20 ± 0.05 |
| | Greedy k | 79.63 ± 0.83 | 86.46 ± 0.27 | 90.09 ± 0.20 | 91.9 ± 0.08 | 92.80 ± 0.08 |
| PruneFuse $p = 0.5$ | Least Conf | 80.92 ± 0.41 | 88.35 ± 0.33 | 91.44 ± 0.15 | 92.77 ± 0.03 | 93.65 ± 0.14 |
| | Entropy | 81.08 ± 0.16 | 88.74 ± 0.10 | 91.33 ± 0.04 | 92.78 ± 0.04 | 93.48 ± 0.04 |
| | Random | 80.43 ± 0.27 | 86.28 ± 0.37 | 88.75 ± 0.17 | 90.36 ± 0.02 | 91.42 ± 0.12 |
| | Greedy k | 79.85 ± 0.68 | 86.96 ± 0.38 | 90.20 ± 0.16 | 91.82 ± 0.14 | 92.89 ± 0.14 |
| PruneFuse $p = 0.6$ | Least Conf | 80.58 ± 0.33 | 87.79 ± 0.20 | 90.94 ± 0.13 | 92.58 ± 0.31 | 93.08 ± 0.42 |
| | Entropy | 80.96 ± 0.16 | 87.89 ± 0.45 | 91.22 ± 0.28 | 92.56 ± 0.19 | 93.19 ± 0.26 |
| | Random | 79.19 ± 0.57 | 85.65 ± 0.29 | 88.27 ± 0.18 | 90.13 ± 0.24 | 91.01 ± 0.28 |
| | Greedy k | 79.54 ± 0.48 | 86.16 ± 0.60 | 89.50 ± 0.29 | 91.35 ± 0.06 | 92.39 ± 0.22 |
| PruneFuse $p = 0.7$ | Least Conf | 80.19 ± 0.45 | 87.88 ± 0.05 | 90.70 ± 0.21 | 92.44 ± 0.24 | 93.40 ± 0.11 |
| | Entropy | 79.73 ± 0.87 | 87.85 ± 0.25 | 90.94 ± 0.29 | 92.41 ± 0.23 | 93.39 ± 0.20 |
| | Random | 78.76 ± 0.23 | 85.50 ± 0.11 | 88.31 ± 0.19 | 89.94 ± 0.24 | 90.87 ± 0.17 |
| | Greedy k | 78.93 ± 0.15 | 85.85 ± 0.41 | 88.96 ± 0.07 | 90.93 ± 0.19 | 92.23 ± 0.08 |
| PruneFuse $p = 0.8$ | Least Conf | 80.11 ± 0.28 | 87.58 ± 0.14 | 90.50 ± 0.08 | 92.42 ± 0.41 | 93.32 ± 0.14 |
| | Entropy | 79.83 ± 1.13 | 87.50 ± 0.54 | 90.52 ± 0.24 | 92.24 ± 0.13 | 93.15 ± 0.10 |
| | Random | 78.77 ± 0.66 | 85.64 ± 0.13 | 88.45 ± 0.33 | 89.88 ± 0.14 | 91.21 ± 0.43 |
| | Greedy k | 78.23 ± 0.37 | 85.59 ± 0.25 | 88.60 ± 0.19 | 90.11 ± 0.11 | 91.31 ± 0.08 |

(a) CIFAR-10 using ResNet-56 architecture.

| **Method** | **Selection Metric** | **Label Budget ($b$)** | | | | |
|---|---|---|---|---|---|---|
| | | **10%** | **20%** | **30%** | **40%** | **50%** |
| Baseline *AL* | Least Conf | 35.99 ± 0.80 | 52.99 ± 0.56 | 59.29 ± 0.46 | 63.68 ± 0.53 | 66.72 ± 0.33 |
| | Entropy | 37.57 ± 0.51 | 52.64 ± 0.76 | 58.87 ± 0.38 | 63.97 ± 0.17 | 66.78 ± 0.27 |
| | Random | 37.06 ± 0.64 | 51.62 ± 0.21 | 58.77 ± 0.65 | 62.05 ± 0.02 | 64.63 ± 0.16 |
| | Greedy k | 38.28 ± 1.11 | 52.43 ± 0.24 | 58.96 ± 0.16 | 63.56 ± 0.30 | 66.30 ± 0.31 |
| PruneFuse $p = 0.5$ | Least Conf | 40.26 ± 0.95 | 53.90 ± 1.06 | 60.80 ± 0.44 | 64.98 ± 0.4 | 67.87 ± 0.17 |
| | Entropy | 38.59 ± 1.67 | 54.01 ± 1.17 | 60.52 ± 0.19 | 64.83 ± 0.27 | 67.67 ± 0.33 |
| | Random | 39.43 ± 0.99 | 54.60 ± 0.64 | 60.13 ± 0.96 | 63.91 ± 0.39 | 66.02 ± 0.3 |
| | Greedy k | 39.83 ± 2.44 | 54.35 ± 0.41 | 60.40 ± 0.23 | 64.22 ± 0.25 | 66.89 ± 0.16 |
| PruneFuse $p = 0.6$ | Least Conf | 37.82 ± 0.83 | 52.65 ± 0.4 | 60.08 ± 0.22 | 63.7 ± 0.25 | 66.89 ± 0.46 |
| | Entropy | 38.01 ± 0.79 | 51.91 ± 0.56 | 59.18 ± 0.31 | 63.53 ± 0.25 | 66.88 ± 0.18 |
| | Random | 38.27 ± 0.81 | 52.85 ± 1.22 | 58.68 ± 0.68 | 62.28 ± 0.22 | 65.2 ± 0.48 |
| | Greedy k | 38.44 ± 0.98 | 52.85 ± 0.74 | 59.36 ± 0.57 | 63.36 ± 0.75 | 66.12 ± 0.38 |
| PruneFuse $p = 0.7$ | Least Conf | 36.76 ± 0.63 | 52.15 ± 0.53 | 59.33 ± 0.17 | 63.65 ± 0.36 | 66.84 ± 0.43 |
| | Entropy | 36.95 ± 1.03 | 50.64 ± 0.33 | 58.45 ± 0.36 | 62.27 ± 0.27 | 65.88 ± 0.28 |
| | Random | 37.30 ± 1.24 | 51.66 ± 0.21 | 58.79 ± 0.13 | 62.67 ± 0.29 | 65.08 ± 0.08 |
| | Greedy k | 38.88 ± 2.18 | 52.02 ± 0.77 | 58.66 ± 0.19 | 61.39 ± 0.11 | 65.28 ± 0.65 |
| PruneFuse $p = 0.8$ | Least Conf | 36.49 ± 0.20 | 50.98 ± 0.54 | 58.53 ± 0.50 | 62.87 ± 0.13 | 65.85 ± 0.32 |
| | Entropy | 36.02 ± 1.30 | 51.23 ± 0.23 | 57.44 ± 0.11 | 62.65 ± 0.46 | 65.76 ± 0.30 |
| | Random | 37.37 ± 0.85 | 52.06 ± 0.47 | 58.19 ± 0.30 | 62.19 ± 0.45 | 64.77 ± 0.29 |
| | Greedy k | 37.04 ± 0.09 | 49.84 ± 0.49 | 56.13 ± 0.20 | 60.24 ± 0.42 | 62.92 ± 0.44 |

(b) CIFAR-100 using ResNet-56 architecture.

Table 8: **Performance Comparison** of Baseline and PruneFuse on CIFAR-10 and CIFAR-100 with ResNet-110 architecture. This table summarizes the test accuracy of final models (original in case of AL and Fused in PruneFuse) for various pruning ratios ($p$), labeling budgets ($b$), and data selection metrics.

| **Method** | **Selection Metric** | **Label Budget ($b$)** | | | | |
|---|---|---|---|---|---|---|
| | | **10%** | **20%** | **30%** | **40%** | **50%** |
| Baseline *AL* | Least Conf. | 80.74 ± 0.04 | 87.80 ± 0.09 | 91.50 ± 0.09 | 93.19 ± 0.14 | 93.68 ± 0.17 |
| | Entropy | 79.81 ± 0.18 | 88.46 ± 0.30 | 91.30 ± 0.15 | 92.83 ±0.30 | 93.47 ± 0.31 |
| | Random | 79.99 ± 0.10 | 85.63 ± 0.03 | 88.07 ± 0.31 | 90.40 ± 0.42 | 91.42 ± 0.26 |
| | Greedy k | 78.69 ± 0.58 | 87.46 ±0.20 | 90.72 ± 0.14 | 92.55 ±0.14 | 93.44 ± 0.07 |
| PruneFuse $p = 0.5$ | Least Conf. | 81.24 ± 0.43 | 88.70 ± 0.15 | 92.02 ± 0.10 | 93.32 ± 0.13 | 94.07 ± 0.06 |
| | Entropy | 81.45 ± 0.39 | 88.90 ± 0.11 | 92.13 ± 0.15 | 93.49 ± 0.16 | 94.07 ± 0.05 |
| | Random | 80.08 ± 0.86 | 86.52 ± 0.14 | 89.48 ± 0.16 | 90.82 ± 0.21 | 91.79 ± 0.04 |
| | Greedy k | 80.40 ± 0.09 | 87.77 ± 0.13 | 90.74 ± 0.09 | 92.48 ± 0.22 | 93.53 ± 0.22 |
| PruneFuse $p = 0.6$ | Least Conf. | 81.12 ± 0.34 | 88.33 ± 0.31 | 91.57 ± 0.03 | 93.25 ± 0.21 | 93.90 ± 0.17 |
| | Entropy | 80.02 ± 0.41 | 88.49 ± 0.18 | 91.51 ± 0.14 | 93.03 ± 0.11 | 93.94 ± 0.12 |
| | Random | 78.55 ± 0.42 | 85.94 ± 0.34 | 88.77 ± 0.10 | 90.66 ± 0.20 | 92.02 ± 0.03 |
| | Greedy k | 79.44 ± 0.28 | 87.05 ± 0.63 | 90.30 ± 0.15 | 92.15 ± 0.12 | 93.22 ± 0.04 |
| PruneFuse $p = 0.7$ | Least Conf. | 79.93 ± 0.06 | 88.04 ± 0.23 | 91.51 ± 0.34 | 92.90 ± 0.02 | 93.82 ± 0.09 |
| | Entropy | 80.16 ± 0.27 | 87.78 ± 0.52 | 91.21 ± 0.13 | 92.99 ± 0.13 | 93.81 ± 0.12 |
| | Random | 79.41 ± 0.36 | 86.14 ± 0.44 | 88.86 ± 0.11 | 90.35 ± 0.08 | 91.35 ± 0.24 |
| | Greedy k | 78.58 ± 0.91 | 86.37 ± 0.36 | 89.70 ± 0.33 | 91.71 ± 0.18 | 92.97 ± 0.10 |
| PruneFuse $p = 0.8$ | Least Conf. | 80.34 ± 0.39 | 88.00 ± 0.13 | 91.22 ± 0.07 | 92.89 ± 0.23 | 93.80 ± 0.23 |
| | Entropy | 79.61 ± 0.35 | 88.12 ± 0.00 | 90.94 ± 0.13 | 92.76 ± 0.14 | 93.54 ± 0.24 |
| | Random | 78.94 ± 0.49 | 86.20 ± 0.10 | 89.11 ± 0.34 | 90.50 ± 0.22 | 91.42 ± 0.23 |
| | Greedy k | 78.41 ± 0.76 | 85.90 ± 0.73 | 89.57 ± 0.51 | 91.38 ± 0.32 | 92.21± 0.22 |

(a) CIFAR-10 using ResNet-110 architecture.

| **Method** | **Selection Metric** | **Label Budget ($b$)** | | | | |
|---|---|---|---|---|---|---|
| | | **10%** | **20%** | **30%** | **40%** | **50%** |
| Baseline *AL* | Least Conf. | 38.61 ±0.32 | 54.47 ±0.56 | 61.46 ±0.25 | 65.96 ±0.48 | 68.91 ± 0.40 |
| | Entropy | 38.00 ± 0.99 | 54.71 ±0.83 | 60.82 ±0.15 | 66.19 ± 0.31 | 68.79 ± 0.50 |
| | Random | 37.88 ± 1.03 | 52.84 ±0.11 | 59.41 ±0.34 | 64.11 ± 0.11 | 67.22 ± 0.36 |
| | Greedy k | 37.41 ± 0.98 | 53.86 ±0.55 | 61.44 ±0.26 | 65.73 ± 0.50 | 68.17 ± 0.46 |
| PruneFuse $p = 0.5$ | Least Conf. | 41.42 ± 0.51 | 55.91 ± 0.36 | 62.43 ± 0.32 | 66.95 ± 0.20 | 69.79 ± 0.26 |
| | Entropy | 40.83 ± 0.59 | 56.29 ± 0.83 | 62.62 ± 0.45 | 66.91 ± 0.02 | 69.96 ± 0.39 |
| | Random | 40.36 ± 0.74 | 55.48 ± 0.25 | 61.14 ± 0.68 | 65.03 ± 0.42 | 67.85 ± 0.53 |
| | Greedy k | 41.22 ± 0.46 | 55.70 ± 0.54 | 62.27 ± 0.02 | 66.20 ± 0.14 | 68.86 ± 0.14 |
| PruneFuse $p = 0.6$ | Least Conf. | 38.52 ± 1.49 | 54.90 ± 0.32 | 61.50 ± 0.77 | 66.14 ± 0.68 | 69.03 ± 0.24 |
| | Entropy | 38.78 ± 1.35 | 53.13 ± 0.30 | 61.42 ± 0.14 | 65.62 ± 0.43 | 68.89 ± 0.09 |
| | Random | 40.24 ± 0.90 | 53.38 ± 0.68 | 59.93 ± 0.12 | 64.70 ± 0.15 | 66.62 ± 0.24 |
| | Greedy k | 39.99 ± 1.56 | 54.91 ± 2.23 | 61.04 ± 0.25 | 64.69 ± 0.63 | 67.60 ± 0.08 |
| PruneFuse $p = 0.7$ | Least Conf. | 37.83 ± 1.02 | 53.08 ± 0.25 | 61.41 ± 0.21 | 65.77 ± 0.43 | 68.03 ± 0.14 |
| | Entropy | 36.53 ± 0.97 | 52.97 ± 0.76 | 59.82 ± 0.63 | 64.97 ± 0.13 | 68.64 ± 0.54 |
| | Random | 39.46 ± 0.59 | 52.89 ± 0.77 | 59.92 ± 0.55 | 63.69 ± 0.25 | 66.30 ± 0.15 |
| | Greedy k | 40.44 ± 0.13 | 52.56 ± 0.28 | 59.83 ± 0.45 | 64.50 ± 0.29 | 66.99 ± 0.50 |
| PruneFuse $p = 0.8$ | Least Conf. | 38.33 ± 0.58 | 52.89 ± 0.49 | 60.08 ± 0.32 | 65.12 ± 0.60 | 68.06 ± 0.56 |
| | Entropy | 35.34 ± 0.98 | 51.88 ± 0.74 | 59.80 ± 0.82 | 64.58 ± 0.43 | 68.02 ± 0.17 |
| | Random | 38.22 ± 0.39 | 53.37 ± 0.72 | 59.84 ± 0.43 | 64.31 ± 0.33 | 67.23 ± 0.25 |
| | Greedy k | 37.72 ± 0.70 | 50.55 ± 1.79 | 57.39 ± 0.93 | 61.79 ± 0.53 | 65.21 ± 0.24 |

(b) CIFAR-100 using ResNet-110 architecture.

Table 9: **Performance Comparison** of Baseline and PruneFuse on CIFAR-10 and CIFAR-100 with ResNet-164 architecture. This table summarizes the test accuracy of final models (original in case of AL and Fused in PruneFuse) for various pruning ratios ($p$), labeling budgets ($b$), and data selection metrics.

| **Method** | **Selection Metric** | **Label Budget ($b$)** | | | | |
|---|---|---|---|---|---|---|
| | | **10%** | **20%** | **30%** | **40%** | **50%** |
| Baseline *AL* | Least Conf. | 81.15 ± 0.52 | 89.4 ± 0.27 | 92.72 ± 0.10 | 94.09 ± 0.14 | 94.63 ± 0.18 |
| | Entropy | 80.99 ± 0.44 | 89.54 ± 0.18 | 92.45 ± 0.16 | 94.06 ± 0.05 | 94.49 ± 0.09 |
| | Random | 80.27 ± 0.18 | 87.00 ± 0.08 | 89.94 ± 0.13 | 91.57 ± 0.09 | 92.78 ± 0.04 |
| | Greedy k | 80.02 ± 0.42 | 88.33 ± 0.47 | 91.76 ± 0.24 | 93.39 ± 0.22 | 94.40 ± 0.18 |
| PruneFuse $p = 0.5$ | Least Conf. | 83.03 ± 0.09 | 90.30 ± 0.06 | 93.00 ± 0.15 | 94.41 ± 0.08 | 94.63 ± 0.13 |
| | Entropy | 82.64 ± 0.22 | 89.88 ± 0.27 | 93.08 ± 0.25 | 94.32 ± 0.12 | 94.90 ± 0.13 |
| | Random | 81.52 ± 0.54 | 87.84 ± 0.15 | 90.14 ± 0.08 | 91.94 ± 0.18 | 92.81 ± 0.12 |
| | Greedy k | 81.70 ± 0.13 | 88.75 ± 0.33 | 91.92 ± 0.07 | 93.64 ± 0.04 | 94.22 ± 0.09 |
| PruneFuse $p = 0.6$ | Least Conf. | 82.86 ± 0.38 | 90.22 ± 0.18 | 93.05 ± 0.10 | 94.27 ± 0.06 | 94.66 ± 0.08 |
| | Entropy | 82.23 ± 0.39 | 90.18 ± 0.11 | 92.91 ± 0.15 | 94.28 ± 0.14 | 94.66 ± 0.14 |
| | Random | 81.14 ± 0.26 | 87.51 ± 0.26 | 90.05 ± 0.20 | 91.82 ± 0.22 | 92.43 ± 0.20 |
| | Greedy k | 81.11 ± 0.10 | 88.41 ± 0.18 | 91.66 ± 0.18 | 92.94 ± 0.12 | 94.17 ± 0.02 |
| PruneFuse $p = 0.7$ | Least Conf. | 82.76 ± 0.29 | 89.89 ± 0.17 | 92.83 ± 0.08 | 94.10 ± 0.08 | 94.69 ± 0.13 |
| | Entropy | 82.59 ± 0.69 | 89.81 ± 0.24 | 92.77 ± 0.07 | 94.20 ± 0.20 | 94.74 ± 0.02 |
| | Random | 80.88 ± 0.38 | 87.54 ± 0.26 | 90.09 ± 0.08 | 91.57 ± 0.26 | 92.64 ± 0.10 |
| | Greedy k | 81.68 ± 0.40 | 88.36 ± 0.56 | 91.64 ± 0.40 | 93.02 ± 0.42 | 93.97 ± 0.51 |
| PruneFuse $p = 0.8$ | Least Conf. | 82.66 ± 0.09 | 89.78 ± 0.27 | 92.64 ± 0.14 | 94.08 ± 0.10 | 94.69 ± 0.17 |
| | Entropy | 82.01 ± 0.88 | 89.77 ± 0.44 | 92.65 ± 0.09 | 94.02 ± 0.17 | 94.60 ± 0.18 |
| | Random | 80.73 ± 0.49 | 87.43 ± 0.44 | 90.08 ± 0.12 | 91.40 ± 0.07 | 92.53 ± 0.18 |
| | Greedy k | 79.66 ± 0.60 | 87.56 ± 0.12 | 90.79 ± 0.07 | 92.30 ± 0.12 | 93.17 ± 0.14 |

(a) CIFAR-10 using ResNet-164 architecture.

| **Method** | **Selection Metric** | **Label Budget ($b$)** | | | | |
|---|---|---|---|---|---|---|
| | | **10%** | **20%** | **30%** | **40%** | **50%** |
| Baseline *AL* | Least Conf | 38.41 ± 0.73 | 51.39 ± 0.30 | 65.53 ± 0.31 | 70.07 ± 0.17 | 73.05 ± 0.11 |
| | Entropy | 36.65 ± 0.76 | 57.58 ± 0.63 | 64.98 ± 0.30 | 69.99 ± 0.17 | 72.90 ± 0.15 |
| | Random | 39.31 ± 1.22 | 57.53 ± 0.26 | 63.84 ± 0.14 | 67.75 ± 0.14 | 70.79 ± 0.07 |
| | Greedy k | 39.76 ± 0.58 | 57.40 ± 0.20 | 65.20 ± 0.31 | 69.25 ± 0.40 | 72.91 ± 0.29 |
| PruneFuse $p = 0.5$ | Least Conf | 42.88 ± 1.11 | 59.31 ± 0.70 | 66.95 ± 0.30 | 71.45 ± 0.42 | 74.32 ± 0.58 |
| | Entropy | 42.99 ± 0.18 | 59.32 ± 1.25 | 66.83 ± 0.29 | 71.18 ± 0.40 | 74.43 ± 0.34 |
| | Random | 43.72 ± 1.05 | 58.58 ± 0.61 | 64.93 ± 0.43 | 68.75 ± 0.57 | 71.63 ± 0.40 |
| | Greedy k | 43.61 ± 0.91 | 58.38 ± 0.24 | 66.04 ± 0.21 | 69.83 ± 0.16 | 73.10 ± 0.39 |
| PruneFuse $p = 0.6$ | Least Conf | 41.86 ± 0.70 | 58.97 ± 0.50 | 66.61 ± 0.39 | 70.59 ± 0.11 | 73.60 ± 0.10 |
| | Entropy | 42.43 ± 0.95 | 58.74 ± 0.80 | 65.97 ± 0.39 | 70.90 ± 0.48 | 73.70 ± 0.09 |
| | Random | 42.53 ± 0.46 | 58.33 ± 0.42 | 65.00 ± 0.26 | 68.55 ± 0.30 | 71.46 ± 0.32 |
| | Greedy k | 42.71 ± 0.91 | 58.41 ± 0.18 | 65.43 ± 0.69 | 69.57 ± 0.14 | 72.49 ± 0.25 |
| PruneFuse $p = 0.7$ | Least Conf | 42.00 ± 0.20 | 57.08 ± 0.36 | 66.41 ± 0.30 | 70.68 ± 0.29 | 73.63 ± 0.29 |
| | Entropy | 41.01 ± 1.66 | 57.45 ± 0.50 | 65.99 ± 0.10 | 70.07 ± 0.54 | 73.45 ± 0.04 |
| | Random | 42.76 ± 1.00 | 57.31 ± 0.07 | 64.12 ± 0.57 | 68.07 ± 0.24 | 70.88 ± 0.25 |
| | Greedy k | 42.42 ± 0.32 | 57.58 ± 0.52 | 65.18 ± 0.51 | 68.55 ± 0.10 | 71.89 ± 0.16 |
| PruneFuse $p = 0.8$ | Least Conf | 41.19 ± 1.07 | 57.98 ± 9.70 | 65.22 ± 0.44 | 70.38 ± 0.22 | 73.17 ± 0.26 |
| | Entropy | 39.78 ± 1.16 | 57.30 ± 0.41 | 65.19 ± 0.63 | 69.40 ± 0.34 | 72.82 ± 0.03 |
| | Random | 42.08 ± 1.55 | 57.23 ± 0.47 | 64.05 ± 0.40 | 67.85 ± 0.19 | 70.62 ± 0.06 |
| | Greedy k | 42.20 ± 1.21 | 57.42 ± 0.50 | 64.53 ± 0.21 | 68.01 ± 0.40 | 71.29 ± 0.14 |

(b) CIFAR-100 using ResNet-164 architecture.

Table 10: **Performance Comparison** of Baseline and PruneFuse on **Tiny ImageNet-200 with ResNet-50 architecture**, including test accuracy and corresponding standard deviations. This table summarizes the test accuracy of final models (original in case of AL and Fused in PruneFuse) for various pruning ratios ($p$) and labeling budgets ($b$).

| **Method** | **Label Budget ($b$)** | | | | |
|---|---|---|---|---|---|
| | **10%** | **20%** | **30%** | **40%** | **50%** |
| Baseline ($AL$) | 14.86 ± 0.11 | 33.62 ± 0.52 | 43.96 ± 0.22 | 49.86 ± 0.56 | 54.65 ± 0.38 |
| PruneFuse ($p = 0.5$) | 18.71 ± 0.21 | 39.70 ± 0.31 | 47.41 ± 0.20 | 51.84 ± 0.10 | 55.89 ± 1.21 |
| PruneFuse ($p = 0.6$) | 19.25 ± 0.72 | 38.84 ± 0.70 | 47.02 ± 0.30 | 52.09 ± 0.29 | 55.29 ± 0.28 |
| PruneFuse ($p = 0.7$) | 18.32 ± 0.95 | 39.24 ± 0.75 | 46.45 ± 0.58 | 52.02 ± 0.65 | 55.63 ± 0.55 |
| PruneFuse ($p = 0.8$) | 18.34 ± 0.93 | 37.86 ± 0.42 | 47.15 ± 0.31 | 51.77 ± 0.40 | 55.18 ± 0.50 |

Table 11: **Performance Comparison** of Baseline and PruneFuse on CIFAR-10 with **MobileNetV2 Architecture**. This table summarizes the test accuracy of final models (original in case of AL and Fused in PruneFuse) for various pruning ratios ($p$) and labeling budgets ($b$).

| **Method** | **Label Budget ($b$)** | | | | |
|---|---|---|---|---|---|
| | **10%** | **20%** | **30%** | **40%** | **50%** |
| Baseline ($AL$) | 81.63 | 89.47 | 91.25 | 91.54 | 91.85 |
| PruneFuse ($p = 0.5$) | **84.49** | **90.07** | **92.63** | **93.49** | **93.55** |
| PruneFuse ($p = 0.6$) | **84.16** | **90.22** | **92.56** | **93.34** | **93.43** |
| PruneFuse ($p = 0.7$) | **84.10** | **90.21** | **92.46** | **93.29** | **93.22** |

Table 12: **Performance Comparison** of Baseline and PruneFuse on CIFAR-10 with **Vision Transformers (ViT)**. This table summarizes the test accuracy of final models (original in case of AL and Fused in PruneFuse) for various pruning ratios ($p$) and labeling budgets ($b$).

| **Method** | **Label Budget ($b$)** | | | | |
|---|---|---|---|---|---|
| | **10%** | **20%** | **30%** | **40%** | **50%** |
| Baseline ($AL$) | 53.63 | 65.62 | 71.09 | 76.86 | 80.59 |
| PruneFuse ($p = 0.5$) | **59.32** | **71.63** | **75.61** | **81.50** | **83.64** |
| PruneFuse ($p = 0.6$) | **57.80** | **70.45** | **75.22** | **80.22** | **82.77** |
| PruneFuse ($p = 0.7$) | **56.17** | **69.25** | **73.87** | **79.47** | **82.15** |

Table 13: **Performance Comparison** of Baseline and PruneFuse on **Amazon Review Polarity Dataset with VDCNN Architecture**. This table summarizes the test accuracy of final models (original in case of AL and Fused in PruneFuse) for various pruning ratios ($p$) and labeling budgets ($b$).

| **Method** | **Label Budget ($b$)** | | | | |
|---|---|---|---|---|---|
| | **10%** | **20%** | **30%** | **40%** | **50%** |
| Baseline ($AL$) | 94.13 | 95.06 | 95.54 | 95.73 | 95.71 |
| PruneFuse ($p = 0.5$) | **94.66** | **95.45** | **95.71** | **95.87** | **95.87** |
| PruneFuse ($p = 0.6$) | **94.62** | **95.38** | **95.69** | **95.82** | **95.88** |
| PruneFuse ($p = 0.7$) | **94.47** | **95.43** | **95.71** | **95.83** | **95.84** |
| PruneFuse ($p = 0.8$) | **94.33** | **95.37** | **95.63** | **95.79** | **95.85** |

### 8.5 Ablation Study of Fusion

The fusion process is a critical component of the PruneFuse methodology, designed to integrate the knowledge gained by the pruned model into the original network. Our experiments reveal that models trained with the fusion process exhibit significantly better performance and faster convergence compared to those trained

Table 14: **Performance Comparison** of Baseline and PruneFuse on **Amazon Review Full Dataset with VDCNN Architecture**. This table summarizes the test accuracy of final models (original in case of AL and Fused in PruneFuse) for various pruning ratios ($p$) and labeling budgets ($b$).

| **Method** | **Label Budget ($b$)** | | | | |
|---|---|---|---|---|---|
| | **10%** | **20%** | **30%** | **40%** | **50%** |
| Baseline ($AL$) | 58.46 | 60.65 | 61.50 | 62.20 | 62.43 |
| PruneFuse ($p = 0.5$) | **59.45** | **61.28** | **62.02** | **62.66** | **62.84** |
| PruneFuse ($p = 0.6$) | **59.28** | **61.14** | **62.08** | **62.62** | **62.81** |
| PruneFuse ($p = 0.7$) | **59.42** | **61.05** | **61.98** | **62.48** | **62.85** |
| PruneFuse ($p = 0.8$) | **59.24** | **61.05** | **61.94** | **62.45** | **62.77** |

Table 15: **Results of CIFAR-10 (in-distribution, ID) and CIFAR-10-C (OOD corruptions) using a ResNet-56 backbone.**

| **Method** | **Label Budget ($b$)** | | | | |
|---|---|---|---|---|---|
| | **10%** | **20%** | **30%** | **40%** | **50%** |
| Baseline ($AL$) (ID) | 48.67 | 58.95 | 65.23 | 72.30 | 73.23 |
| PruneFuse ($p = 0.5$) (ID) | **51.20** | **64.68** | **67.52** | **73.28** | **77.71** |
| Baseline ($AL$) (OOD) | 42.95 | 48.56 | 53.62 | 57.27 | 58.32 |
| PruneFuse ($p = 0.5$) (OOD) | **44.58** | **52.44** | **54.60** | **58.36** | **63.37** |

without fusion. By initializing the original model with the weights from the trained pruned model, the fused model benefits from an optimized starting point, which enhances its learning efficiency and generalization capability. Fig. 5, 6 and 7 illustrates the training trajectories and accuracy improvements when fusion takes places, demonstrating the tangible benefits of this initialization. These results underscore the importance of the fusion step in maximizing the overall performance of the PruneFuse framework.

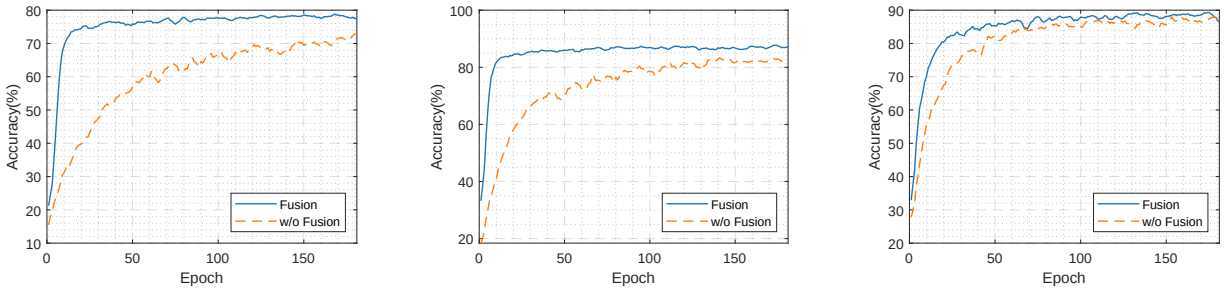


(a) $p = 0.5$, $b = 10\%$ (b) $p = 0.5$, $b = 30\%$ (c) $p = 0.5$, $b = 50\%$

Figure 5: **Ablation Study of Fusion on PruneFuse** ($p = 0.5$). Experiments are performed on ResNet-56 architecture with CIFAR-10.

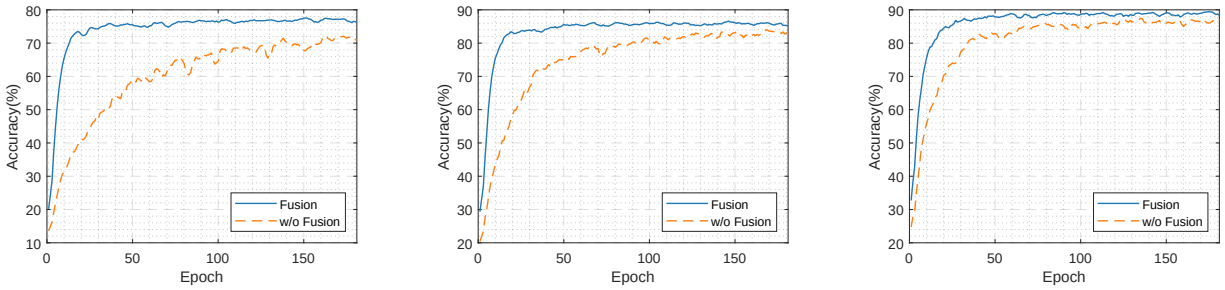


(a) $p = 0.6$, $b = 10\%$ (b) $p = 0.6$, $b = 30\%$ (c) $p = 0.6$, $b = 50\%$

Figure 6: **Ablation Study of Fusion on PruneFuse** ($p = 0.6$). Experiments are performed on ResNet-56 architecture with CIFAR-10.

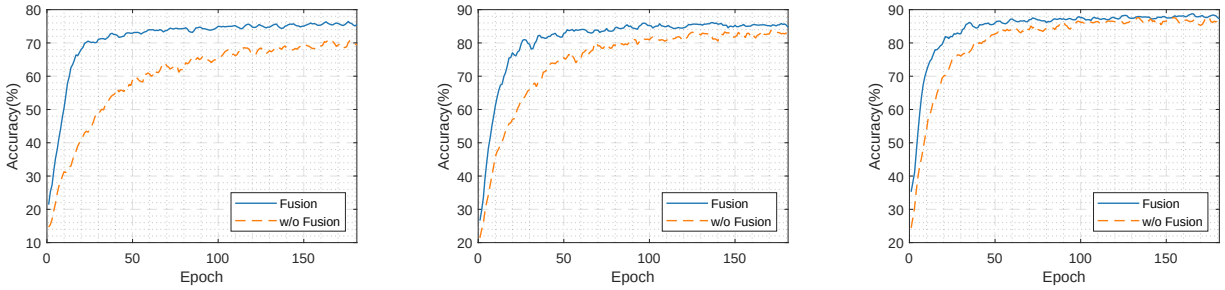


(a) $p = 0.7$, $b = 10\%$ (b) $p = 0.7$, $b = 30\%$ (c) $p = 0.7$, $b = 50\%$

Figure 7: **Ablation Study of Fusion on PruneFuse** ($p = 0.7$). Experiments are performed on ResNet-56 architecture with CIFAR-10.

### 8.6 Ablation Study of Knowledge Distillation in PruneFuse

Table 16 demonstrates the effect of Knowledge Distillation on the PruneFuse technique relative to the baseline Active Learning (AL) method across various experimental configurations and label budgets on CIFAR-10 and CIFAR-100 datasets, using different ResNet architectures. The results indicate that PruneFuse consistently outperforms the baseline method, both with and without incorporating Knowledge Distillation (KD) from a trained pruned model. This superior performance is attributed to the innovative fusion strategy inherent to PruneFuse, where the original model is initialized using weights from a previously trained pruned model. The proposed approach gives the fused model an optimized starting point, enhancing its ability to learn more efficiently and generalize better. The impact of this strategy is evident across different label budgets and architectures, demonstrating its effectiveness and robustness.

### 8.7 Comparison with SVP

Table 18 delineates a performance comparison of PruneFuse with SVP techniques, across various labeling budgets $b$ for the efficient training of a Target Model (ResNet-56). SVP employs a ResNet-20 as its data selector, with a model size of 0.26 M. In contrast, PruneFuse uses a 50% pruned ResNet-56, reducing its data selector size to 0.21 M. Performance metrics show that as the label budget increases from 10% to 50%, the PruneFuse consistently outperforms SVP across all label budgets. Specifically on the target model, PruneFuse initiates at an accuracy of 82.68% with a 10% label budget and peaks at 93.69% accuracy at a 50% budget, whereas SVP achieves 80.76% at 10% label budget and achieves 92.95% accuracy at 50%. Notably, while the data selector of PruneFuse achieves a lower accuracy of 90.31% at $b = 50\%$ compared to SVP's 91.61%, the target model utilizing PruneFuse-selected data attains a superior accuracy of 93.69%, relative to 92.95% for the SVP-selected data. This disparity underscores the distinct operational focus of the

Table 16: Ablation Study of Knowledge Distillation on PruneFuse presented in a, b, and c with different architectures and datasets.

| Method | Selection Metric | Label Budget ($b$) | | | | |
|---|---|---|---|---|---|---|
| | | **10%** | **20%** | **30%** | **40%** | **50%** |
| Baseline *AL* | Least Conf | 80.53 | 87.74 | 90.85 | 92.24 | 93.00 |
| | Entropy | 80.14 | 87.63 | 90.80 | 92.51 | 92.98 |
| | Random | 78.55 | 85.26 | 88.13 | 89.81 | 91.20 |
| | Greedy k | 79.63 | 86.46 | 90.09 | 91.90 | 92.80 |
| PruneFuse $p = 0.5$ (without KD) | Least Conf | **81.08** | **88.71** | **91.24** | **92.68** | **93.46** |
| | Entropy | **80.80** | **88.08** | **90.98** | **92.74** | **93.43** |
| | Random | **80.11** | **85.78** | **88.81** | **90.20** | 91.10 |
| | Greedy k | **80.07** | **86.70** | 89.93 | 91.72 | 92.67 |
| PruneFuse $p = 0.5$ (with KD) | Least Conf | **80.92** | **88.35** | **91.44** | **92.77** | **93.65** |
| | Entropy | **81.08** | **88.74** | **91.33** | **92.78** | **93.48** |
| | Random | **80.43** | **86.28** | **88.75** | **90.36** | **91.42** |
| | Greedy k | **79.85** | **86.96** | **90.20** | 91.82 | **92.89** |

(a) CIFAR-10 using ResNet-56 architecture.

| Method | Selection Metric | Label Budget ($b$) | | | | |
|---|---|---|---|---|---|---|
| | | **10%** | **20%** | **30%** | **40%** | **50%** |
| Baseline *AL* | Least Conf | 81.15 | 89.4 | 92.72 | 94.09 | 94.63 |
| | Entropy | 80.99 | 89.54 | 92.45 | 94.06 | 94.49 |
| | Random | 80.27 | 87.00 | 89.94 | 91.57 | 92.78 |
| | Greedy k | 80.02 | 88.33 | 91.76 | 93.39 | 94.40 |
| PruneFuse $p = 0.5$ (without KD) | Least Conf | **83.82** | **90.26** | **93.15** | **94.34** | **94.90** |
| | Entropy | **82.72** | **90.42** | **93.18** | **94.68** | **95.00** |
| | Random | **81.94** | **88.04** | **90.37** | **91.93** | 92.67 |
| | Greedy k | **81.99** | **89.04** | **92.14** | **93.40** | **94.44** |
| PruneFuse $p = 0.5$ (with KD) | Least Conf. | **83.03** | **90.30** | **93.00** | **94.41** | **94.63** |
| | Entropy | **82.64** | **89.88** | **93.08** | **94.32** | **94.90** |
| | Random | **81.52** | **87.84** | **90.14** | **91.94** | **92.81** |
| | Greedy k | **81.70** | **88.75** | **91.92** | **93.64** | 94.22 |

(b) CIFAR-10 using ResNet-164 architecture.

| Method | Selection Metric | Label Budget ($b$) | | | | |
|---|---|---|---|---|---|---|
| | | **10%** | **20%** | **30%** | **40%** | **50%** |
| Baseline *AL* | Least Conf | 35.99 | 52.99 | 59.29 | 63.68 | 66.72 |
| | Entropy | 37.57 | 52.64 | 58.87 | 63.97 | 66.78 |
| | Random | 37.06 | 51.62 | 58.77 | 62.05 | 64.63 |
| | Greedy k | 38.28 | 52.43 | 58.96 | 63.56 | 66.30 |
| PruneFuse $p = 0.5$ (without KD) | Least Conf | **39.27** | **54.25** | **60.6** | **64.17** | **67.49** |
| | Entropy | **37.43** | **52.57** | **60.57** | **64.44** | **67.31** |
| | Random | **40.07** | **52.83** | **59.93** | **63.06** | **65.41** |
| | Greedy k | **39.25** | **52.43** | **59.94** | **63.94** | **66.56** |
| PruneFuse $p = 0.5$ (with KD) | Least Conf | **40.26** | **53.90** | **60.80** | **64.98** | **67.87** |
| | Entropy | **38.59** | **54.01** | **60.52** | **64.83** | **67.67** |
| | Random | **39.43** | **54.60** | **60.13** | **63.91** | **66.02** |
| | Greedy k | **39.83** | **54.35** | **60.40** | **64.22** | **66.89** |

(c) CIFAR-100 using ResNet-56 architecture.

data selectors: PruneFuse's selector is optimized for enhancing the target model's performance, rather than its own accuracy. Fig. 8(a) and (b) show that target models ResNet-14 and ResNet-20, when trained with the data selectors of the PruneFuse achieve significantly higher accuracy while using significantly less number of parameters compared to SVP. These results indicate that the proposed approach does not require an additional architecture for designing the data selector; it solely needs the target model (e.g. ResNet-14). In contrast, SVP necessitates both the target model (ResNet-14) and a smaller model (ResNet-8) that functions as a data selector.

Table 17: Comparison of SVP and PruneFuse on Small Models.

| Techniques | Model | Architecture | Params (Million) | Label Budget ($b$) | | | | |
|---|---|---|---|---|---|---|---|---|
| | | | | 10% | 20% | 30% | 40% | 50% |
| SVP | Data Selector | ResNet-8 | 0.074 | 77.85 | 83.35 | 85.43 | 86.83 | 86.90 |
| | Target | ResNet-20 | 0.26 | 80.18 | 86.34 | 89.22 | 90.75 | 91.88 |
| PruneFuse | Data Selector | ResNet-20 ($p = 0.5$) | **0.066** | 76.58 | 83.41 | 85.83 | 87.07 | 88.06 |
| | Target | ResNet-20 | 0.26 | **80.25** | **87.57** | **90.20** | **91.70** | **92.29** |

Table 17 demonstrates the performance comparison of PruneFuse and SVP for small model architecture ResNet-20 on CIFAR-10. SVP achieves 91.88% performance accuracy by utilizing the data selector having 0.074 M parameters whereas PruneFuse outperforms SVP by achieving 92.29% accuracy with a data selector of 0.066 M parameters.

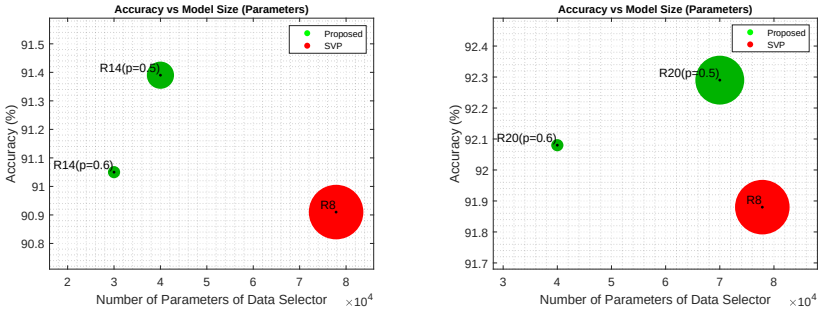


(a) Target Model = ResNet-14 (b) Target Model = ResNet-20

Figure 8: **Comparison of PruneFuse with SVP.** Scatter plot shows final accuracy on target model against the model size for different ResNet models on CIFAR-10, $b = 50\%$. (a) shows ResNet-14 (with $p = 0.5$ and $p = 0.6$) and ResNet-8 models are used as data selectors for PruneFuse and SVP, respectively. While in (b), PruneFuse utilizes ResNet20 (i.e. $p = 0.5$ and $p = 0.6$) and SVP utilizes ResNet-8 models.

Table 18: Comparison with SVP.

| Method | Model | Architecture | Params (Million) | Label Budget ($b$) | | | | |
|---|---|---|---|---|---|---|---|---|
| | | | | 10% | 20% | 30% | 40% | 50% |
| SVP | Data Selector | ResNet-20 | 0.26 | 81.07 | 86.51 | 89.77 | 91.08 | 91.61 |
| | Target | ResNet-56 | 0.85 | 80.76 | 87.31 | 90.77 | 92.59 | 92.95 |
| PruneFuse | Data Selector | ResNet-56 ($p = 0.5$) | **0.21** | 78.62 | 84.92 | 88.17 | 89.93 | 90.31 |
| | Target | ResNet-56 | 0.85 | **82.68** | **88.97** | **91.63** | **93.24** | **93.69** |

### 8.8 Ablation Study on the Number of Selected Data Points ($k$)

Table 19 and 20 present ablation studies analyzing the effect of varying $k$ on the performance of PruneFuse with $T_{sync} = 0$ and $T_{sync} = 1$, respectively, on CIFAR-10 using the ResNet-56 architecture and least confidence as the selection metric. The results demonstrate that the choice of $k$ significantly impacts the quality of data selection and the final performance of the model. As $k$ increases, the selected subset quality diminishes as can be seen by comparing performance of the target network in both tables. This study highlights the importance of tuning $k$ to achieve an optimal trade-off between computational efficiency and model accuracy.

Table 19: **Ablation study of** $k$ on Cifar-10 using ResNet-56 architecture and least confidence as a selection matric.

(a) $k = 7.5K$.

| **Method** | **Label Budget** ($b$) | | | | |
|---|---|---|---|---|---|
| | **15%** | **30%** | **45%** | **60%** | **75%** |
| Baseline ($AL$) | 84.63 | 90.59 | 92.77 | 93.12 | 93.94 |
| PruneFuse ($p = 0.5$) | **85.80** | **91.13** | **93.72** | **93.84** | **94.10** |

(b) $k = 5K$.

| **Method** | **Label Budget** ($b$) | | | | |
|---|---|---|---|---|---|
| | **10%** | **20%** | **30%** | **40%** | **50%** |
| Baseline ($AL$) | 80.53 | 87.74 | 90.85 | 92.24 | 93.00 |
| PruneFuse ($p = 0.5$) | **80.92** | **88.35** | **91.44** | **92.77** | **93.65** |

Table 20: **Ablation study of** $k$ on Cifar-10 using ResNet-56 with $p = 0.5$ and $T_{sync} = 1$.

| **Method** | **Selection** | **Label Budget** ($b$) | | | **Selection** | **Label Budget** ($b$) | | |
|---|---|---|---|---|---|---|---|---|
| | **Size** (k) | **20%** | **40%** | **60%** | **Size** (k) | **20%** | **40%** | **60%** |
| **Baseline** ($AL$) | 5,000 | 88.51 | 93.04 | 93.83 | 10,000 | 86.92 | 92.51 | 93.81 |
| **PruneFuse** | 5,000 | **88.52** | **93.15** | **93.90** | 10,000 | **87.49** | **93.11** | **94.04** |

## 8.9 Impact of Early Stopping on Performance

Table 21 explores the effect of utilizing an early stopping strategy alongside PruneFuse ($p = 0.5$) on CIFAR-10 with the ResNet-56 architecture. The results indicate that early stopping not only reduces training time of the fused model but also maintains comparable performance to fully trained models. This highlights the compatibility of PruneFuse with training efficiency techniques such as early stopping and showcases how the expedited convergence enabled by the fusion process further enhances its practicality, particularly in resource-constrained environments.

Table 21: **Performance Comparison** when Early Stopping strategy is utilized alongside PruneFuse ($p = 0.5$). Experiments are performed with Resnet-56 on CIFAR-10.

| **Method** | **Epochs** | **Label Budget** ($b$) | | | | |
|---|---|---|---|---|---|---|
| | | **10%** | **20%** | **30%** | **40%** | **50%** |
| Least Conf. | 181 | 80.92±0.409 | 88.35±0.327 | 91.44±0.148 | 92.77±0.026 | 93.65±0.141 |
| | 110 | 80.51±0.375 | 87.64±0.222 | 90.79±0.052 | 92.11±0.154 | 93.00±0.005 |
| Entropy | 181 | 81.08±0.155 | 88.74±0.103 | 91.33±0.045 | 92.78±0.045 | 93.48±0.042 |
| | 110 | 80.51±0.401 | 87.46±0.416 | 90.97±0.116 | 92.2±0.108 | 92.88±0.264 |
| Random | 181 | 80.43±0.273 | 86.28±0.367 | 88.75±0.17 | 90.36±0.022 | 91.42±0.125 |
| | 110 | 79.29±0.355 | 84.99±0.156 | 87.86±0.323 | 89.99±0.090 | 90.85±0.012 |
| Greedy k. | 181 | 79.85±0.676 | 86.96±0.385 | 90.20±0.164 | 91.82±0.136 | 92.89±0.144 |
| | 110 | 79.36±0.274 | 86.36±0.455 | 89.67±0.319 | 91.19±0.302 | 91.91±0.021 |

## 8.10 Performance Comparison Across Architectures and Datasets

In Table 22, we present the performance comparison of Baseline and PruneFuse across various architectures and datasets. These results demonstrate the adaptability of PruneFuse to different network architectures, including ResNet-18, ResNet-50, and Wide-ResNet (W-28-10), as well as datasets such as CIFAR-10, CIFAR-100, and ImageNet. The experiments confirm that PruneFuse consistently improves performance over the baseline, highlighting its generalizability and robustness across diverse scenarios.

Table 22: **Performance Comparison of Baseline and PruneFuse** presented in a, b, and b with different architectures and datasets.

| Method | Label Budget ($b$) | | | | |
|---|---|---|---|---|---|
| | **10%** | **20%** | **30%** | **40%** | **50%** |
| Baseline ($AL$) | 83.12 | 90.07 | 92.71 | 94.07 | 94.81 |
| PruneFuse ($p = 0.5$) | **83.29** | **90.56** | **93.17** | **94.56** | **95.08** |

(a) ResNet-18 architecture on CIFAR-10.

| Method | Label Budget ($b$) | | | | |
|---|---|---|---|---|---|
| | **10%** | **20%** | **30%** | **40%** | **50%** |
| Baseline ($AL$) | 84.74 | 91.48 | 94.17 | 95.24 | 95.75 |
| PruneFuse ($p = 0.5$) | **85.65** | **92.27** | **94.65** | **95.73** | **96.24** |

(b) Wide-ResNet architecture on CIFAR-10.

| Method | Label Budget ($b$) | | | | |
|---|---|---|---|---|---|
| | **10%** | **20%** | **30%** | **40%** | **50%** |
| Baseline ($AL$) | 52.97 | 64.52 | 69.30 | 71.98 | 73.56 |
| PruneFuse ($p = 0.5$) | **55.03** | **65.12** | **69.72** | **72.07** | **73.86** |

(c) ResNet-50 architecture on ImageNet-1K.

### 8.11 Performance at Lower Pruning Rates

Table 23 provides a performance comparison of Baseline and PruneFuse with a lower pruning rate of $p = 0.4$ on CIFAR-10 and CIFAR-100 using the ResNet-56 architecture. Least Confidence and Entropy were used as selection metrics for these experiments. The results show that even at a lower pruning rate, PruneFuse effectively selects high-quality data subsets, maintaining strong performance in both datasets. These findings validate the method's effectiveness across different pruning rates.

Table 23: **Performance Comparison of Baseline and PruneFuse**($p = 0.4$) on Cifar-10 and Cifar-100 using ResNet-56 architecture.

| Method | Selection Metric | Label Budget ($b$) | | | | |
|---|---|---|---|---|---|---|
| | | **10%** | **20%** | **30%** | **40%** | **50%** |
| Baseline ($AL$) | Least Confidence | 80.53 | 87.74 | 90.85 | 92.24 | 93.00 |
| | Entropy | 80.14 | 87.63 | 90.80 | 92.51 | 92.98 |
| PruneFuse ($p = 0.4$) | Least Confidence | **81.12** | **88.16** | **91.35** | **92.89** | **93.20** |
| | Entropy | **80.94** | **88.27** | **91.09** | **92.73** | **93.38** |

(a) CIFAR-10

| Method | Selection Metric | Label Budget ($b$) | | | | |
|---|---|---|---|---|---|---|
| | | **10%** | **20%** | **30%** | **40%** | **50%** |
| Baseline ($AL$) | Least Confidence | 35.99 | 52.99 | 59.29 | 63.68 | 66.72 |
| | Entropy | 37.57 | 52.64 | 58.87 | 63.97 | 66.78 |
| PruneFuse ($p = 0.4$) | Least Confidence | **38.73** | **54.35** | **60.75** | **64.80** | **67.08** |
| | Entropy | **38.35** | **54.19** | **60.79** | **65.00** | **67.47** |

(b) CIFAR-100

### 8.12 Comparison with Recent Coreset Selection Techniques

Table 24 compares the performance of Baseline (Coreset Selection) and PruneFuse ($p = 0.5$) using various recent selection metrics, including Forgetting Events (Toneva et al., 2019), Moderate (Xia et al., 2022), and CSS (Zheng et al., 2022) on the CIFAR-10 dataset with the ResNet-56 architecture.

To incorporate these recent score metrics, which are specifically designed for coreset-based selection, we utilized the coreset task setup. In this setup, the network is first trained on the entire dataset to identify a representative subset of data (coreset) based on the selection metric. The accuracy of the target model trained on the selected coreset is then reported. The results demonstrate that PruneFuse seamlessly integrates with these advanced selection metrics, achieving competitive or superior performance compared to the baseline while maintaining computational efficiency. This highlights the versatility of PruneFuse in adapting to and enhancing existing coreset selection techniques.

Table 24: **Performance Comparison of Baseline (Coreset) and PruneFuse ($p = 0.5$) for Various selection metrics** including Forgetting Events (Toneva et al., 2019), Moderate (Xia et al., 2023), and CSS (Zheng et al., 2023) on Cifar-10 dataset using ResNet-56 architecture.

| Method | Selection Metric | Data Selector's Params | Target Model's Params | Accuracy ($b = 25\%$) |
|---|---|---|---|---|
| **Baseline** | Entropy | 0.85 Million | 0.85 Million | 86.13 |
| | Least Confidence | | | 86.50 |
| | Forgetting Events | | | 86.01 |
| | Moderate | | | 86.27 |
| | CSS | | | 87.21 |
| **PruneFuse** | Entropy | 0.21 Million | 0.85 Million | **86.71** |
| | Least Confidence | | | **86.68** |
| | Forgetting Events | | | **87.84** |
| | Moderate | | | **87.63** |
| | CSS | | | **88.85** |

## 8.13 Effect of Various Pruning Strategies and Criteria

In Table 25, we evaluate the impact of different pruning techniques (e.g., static pruning, dynamic pruning) and pruning criteria (e.g., L2 norm, GroupNorm Importance, LAMP Importance [Fang et al. (2023)]) on the performance of PruneFuse ($p = 0.5$) on CIFAR-10 using the ResNet-56 architecture.

Static pruning involves pruning the entire network at once at the start of training, whereas dynamic pruning incrementally prunes the network in multiple steps during training. In our implementation of dynamic pruning, the network is pruned in five steps over the course of 20 epochs.

The results demonstrate that PruneFuse is highly adaptable to various pruning strategies, consistently maintaining strong performance in data selection tasks. This flexibility underscores the robustness of the framework across different pruning approaches and criteria.

Table 25: **Effect of different Pruning Techniques and Pruning Criteria** on PruneFuse ($p = 0.5$) on Cifar-10 dataset with ResNet-56 architecture.

| Method | Pruning Criteria | Label Budget ($b$) | | | | |
|---|---|---|---|---|---|---|
| | | **10%** | **20%** | **30%** | **40%** | **50%** |
| **Baseline (AL)** | - | 80.53 | 87.74 | 90.85 | 92.24 | 93.00 |
| **PruneFuse** ($T_{sync} = 0$) (Dynamic Pruning) | Magnitude Imp. | 79.73 | 87.16 | **91.08** | **92.29** | **93.19** |
| | GroupNorm Imp. | 80.10 | **88.25** | **91.01** | **92.25** | **93.74** |
| | LAMP Imp. | **81.51** | 87.45 | 90.64 | **92.41** | **93.25** |
| **PruneFuse** ($T_{sync} = 0$) (Static Pruning) | Magnitude Imp. | **80.92** | **88.35** | **91.44** | **92.77** | **93.65** |
| | GroupNorm Imp. | **80.84** | **88.20** | **91.19** | **93.01** | **93.03** |
| | LAMP Imp. | **81.10** | **88.37** | **91.32** | **93.02** | **93.08** |
| **PruneFuse** ($T_{sync} = 1$) (Static Pruning) | Magnitude Imp. | **81.23** | **88.52** | **91.76** | **93.15** | **93.78** |
| | GroupNorm Imp. | **81.09** | **88.77** | **91.77** | **93.19** | **93.68** |
| | LAMP Imp. | **81.86** | **88.51** | **92.10** | **93.02** | **93.63** |

## 8.14 Runtime Comparison of Data Selector Networks and Detailed Breakdown of the Training Runtime for each Component of PruneFuse

Table 26 compares the training runtimes of the data selector network (pruned network for PruneFuse and dense network for the baseline) across various network architectures. The reported times correspond to the

training phase of the data selector network prior to the final selection of the subset (at $b = 50\%$, label budget). Note that the variation in runtimes across different datasets is due to the experiments being conducted on different servers, each equipped with specific GPUs (e.g., 2080Ti, 3090, or A100). The results show that PruneFuse significantly reduces training time due to the efficiency of the pruned network as compared to baseline, making it well suited for resource-constrained environments.

Table 27 provides a detailed breakdown of the training run time for each component of PruneFuse, including the data selector training time, the selection time, and the target network training time. These measurements offer a comprehensive view of the computational requirements of PruneFuse, demonstrating its efficiency compared to the baseline methods. The breakdown highlights that the pruned network and the fusion process contribute to significant computational savings without compromising performance.

Table 26: **Training Runtime** of data selector network i.e. pruned network in the case of PruneFuse and dense network for baseline, for various network architectures. The reported time is the training time when the network is trained before selecting final subset of the data ($b = 50\%$).

| **Datasets** | **Data Selectors** (Selection Models) | **Training Runime** (Minutes) |
|---|---|---|
| **CIFAR-10** | ResNet-56 (Baseline) | 127.67 |
| | ResNet-56 (PruneFuse ($p = 0.5$)) | **72.55** |
| | ResNet-56 (PruneFuse ($p = 0.8$)) | **67.23** |
| | ResNet-18 (Baseline) | 85.68 |
| | ResNet-18 (PruneFuse ($p = 0.5$)) | **61.15** |
| | Wide ResNet (Baseline) | 122.43 |
| | Wide ResNet (PruneFuse ($p = 0.5$)) | **75.48** |
| **CIFAR-100** | ResNet-164 (Baseline) | 129.23 |
| | ResNet-164 (PruneFuse ($p = 0.5$)) | **83.52** |
| | ResNet-164 (PruneFuse ($p = 0.8$)) | **78.55** |
| | ResNet-110 (Baseline) | 95.80 |
| | ResNet-110 (PruneFuse ($p = 0.5$)) | **80.42** |
| | ResNet-110 (PruneFuse ($p = 0.8$)) | **69.50** |
| **TinyImagenet-200** | ResNet-50 (Baseline) | 248.48 |
| | ResNet-50 (PruneFuse ($p = 0.5$)) | **147.47** |
| | ResNet-50 (PruneFuse ($p = 0.8$)) | **94.42** |
| **ImageNet-1K** | Resnet-50 (Baseline) | 2081.3 |
| | ResNet-50 (PruneFuse ($p = 0.5$)) | **951.17** |

Table 27: **Detailed Training time of Baseline and PruneFuse($p = 0.5$)** for TinyImageNet-200 for Resnet-50 using Least Confidence as selection metric.

| **Datasets** | **Label Budget** ($b$) | **Data Selectors** (Training Time ) (Minutes) | **Data Selection Time** (Minutes) | **Target Model** (Training Time) (Minutes) |
|---|---|---|---|---|
| **Baseline (AL)** | 10% | 48.80 | 4.43 | 48.80 |
| | 20% | 99.23 | 3.50 | 99.23 |
| | 30% | 145.32 | 3.15 | 145.32 |
| | 40% | 195.38 | 2.72 | 195.38 |
| | 50% | 248.48 | 2.38 | 248.48 |
| **PruneFuse** | 10% | **32.17** | **1.57** | 49.50 |
| | 20% | **61.70** | **1.67** | 99.99 |
| | 30% | **88.53** | **1.52** | 146.25 |
| | 40% | **117.10** | **1.37** | 196.28 |
| | 50% | **147.47** | **1.18** | 249.58 |

Table 28: **Results with ResNet20 and ResNet56 on CIFAR-10 (Least Confidence & Entropy) using ALSE Jung et al. (2023).**

| Model / Selection Metric | Method with ALSE | 10% | 20% | 30% | 40% | 50% |
|---|---|---|---|---|---|---|
| ResNet20 / Least Conf. | Baseline | 80.24 | 86.28 | 89.07 | 90.27 | 91.09 |
| | PruneFuse ($p = 0.4$) | **81.05** | **86.82** | **90.02** | **90.89** | **91.54** |
| | PruneFuse ($p = 0.5$) | **80.72** | **86.65** | **89.79** | **90.79** | **91.51** |
| | PruneFuse ($p = 0.6$) | **80.53** | **86.68** | **89.56** | **90.81** | **91.32** |
| ResNet56 / Least Conf. | Baseline | 80.73 | 88.13 | 90.99 | 92.58 | 93.13 |
| | PruneFuse ($p = 0.4$) | **80.86** | **88.28** | **91.36** | **93.15** | **93.44** |
| | PruneFuse ($p = 0.5$) | **80.80** | **88.17** | **91.43** | **93.02** | **93.19** |
| | PruneFuse ($p = 0.6$) | **80.76** | **87.80** | **91.29** | **92.73** | **93.20** |
| ResNet20 / Entropy | Baseline | 80.12 | 86.01 | 88.96 | 90.68 | 91.21 |
| | PruneFuse ($p = 0.4$) | **80.64** | **86.99** | **89.65** | **91.27** | **91.46** |
| | PruneFuse ($p = 0.5$) | **80.39** | **86.59** | **89.49** | **90.97** | **91.42** |
| | PruneFuse ($p = 0.6$) | **80.29** | **86.24** | **88.94** | **90.75** | **91.24** |
| ResNet56 / Entropy | Baseline | 80.59 | 88.11 | 90.88 | 92.52 | 93.06 |
| | PruneFuse ($p = 0.4$) | **81.05** | **88.49** | **91.38** | **92.95** | **93.44** |
| | PruneFuse ($p = 0.5$) | **80.97** | **88.37** | **91.31** | **92.87** | **93.32** |
| | PruneFuse ($p = 0.6$) | **80.77** | **88.09** | **91.08** | **92.71** | **93.20** |